Zoological Journal of the Linnean Society, 2019, **187**, 622–660. With 17 figures.

Homoplasy and extinction: the phylogeny of cassidulid echinoids (Echinodermata)

CAMILLA SOUTO[1,2,3,*], RICH MOOI[2], LUCIANA MARTINS[3,4], CARLA MENEGOLA[3,5] and CHARLES R. MARSHALL[1]

[1]*Department of Integrative Biology and University of California Museum of Paleontology, University of California, Berkeley, CA 94720-4780, USA*
[2]*Department of Invertebrate Zoology and Geology, California Academy of Sciences, 55 Music Concourse Drive, San Francisco, CA 94118, USA*
[3]*Programa de Pós-Graduação em Diversidade Animal, Instituto de Biologia, Universidade Federal da Bahia, Av. Barão de Jeremoabo s/n, Campus Universitário, Ondina, Salvador, BA 40170-290, Brazil*
[4]*Museu de Zoologia, Universidade de São Paulo, PO Box 42494, São Paulo, SP 04218-970, Brazil*
[5]*Centro de Estudos Costeiros, Limnológicos e Marinhos (CECLIMAR), Universidade Federal do Rio Grande do Sul, Campus Litoral Norte, Imbé, RS 95625-000, Brazil*

Received 1 February 2019; revised 16 May 2019; accepted for publication 9 June 2019

Inclusion of fossils can be crucial to address evolutionary questions, because their unique morphology, often drastically modified in recent species, can improve phylogenetic resolution. We performed a cladistic analysis of 45 cassidulids with 98 characters, which resulted in 24 most parsimonious trees. The strict consensus recovers three major cassiduloid clades, and the monophyly of the family Cassidulidae is not supported. Ancillary analyses to determine the sensitivity of the phylogeny to missing data do not result in significantly different topologies. The taxonomic implications of these results, including the description of a new cassiduloid family and the evolution of some morphological features, are discussed. Cassiduloids (as defined here) most probably originated in the Early Cretaceous, and their evolutionary history has been dominated by high levels of homoplasy and a dearth of unique, novel traits. Despite their high diversity during the Palaeogene, there are only seven extant cassiduloid species, and three of these are relicts of lineages dating back to the Eocene. Future studies of the biology of these poorly known species, some of which brood their young, will yield further insights into the evolutionary history of this group.

ADDITIONAL KEYWORDS: Cassiduloida – classification – Echinoidea – fossil – missing data – Neognathostomata – new taxon – phylogenetic systematics – relict species – taxonomy.

INTRODUCTION

Cassiduloids (from here onwards, *sensu* Kier, 1962, unless stated otherwise) are irregular echinoids that originated during the Marine Mesozoic Revolution (Kier, 1974; Vermeij, 1977), when the evolution of traits that permitted infaunalization (e.g. bilateralization of the body, increased number of spines, evolution of petals and migration of the periproct away from the apical system) opened up possibilities of avoiding epifaunal predation and for exploring a new ecological space (Barras, 2008; Boivin *et al.*, 2018). The rich fossil record of cassiduloids indicates that they thrived early in their evolution and survived the end-Cretaceous mass extinction (Smith & Jeffery, 1998), reaching their highest taxonomic diversity during the Eocene (~56–40 Mya) when they composed > 40% of the echinoid diversity (Kier, 1974). Since then, their diversity has been declining, and today they represent only 3% (~30 species) of all living echinoids (Mooi, 1990b). Explanations for this demise have included the lack of morphological innovation, competition with clypeasteroids and spatangoids, Cenozoic cooling and

*Corresponding author. E-mail: csouto@berkeley.edu
[Version of Record, published online 14 August 2019; http://zoobank.org/urn:lsid:zoobank.org:pub:F724DA40-7ADE-47F8-8691-3123E89051A4]

stochastic events (Suter, 1988; McKinney & Oyen, 1989; Wagner, 2000).

Taxonomically, the order Cassiduloida has traditionally been a 'trash can' among the irregular echinoids. The lack of unifying characteristics (synapomorphies) means that almost any irregular echinoid without a plastron or a clypeasteroid shape could be assigned to the group. As a result, proposed classification schemes include artificial families, sometimes even explicitly acknowledged as such by their authors [e.g. Cassidulidae and Echinobrissidae (Mortensen, 1948a) and Pliolampadidae (Kier, 1962)]. Kier's (1962) monograph was a great advance for cassiduloid studies, but subsequent phylogenetic analyses have shown that nearly all ten families proposed by him are not monophyletic, nor is the order Cassiduloida (*sensu* Kier, 1962) monophyletic (Suter, 1994a, b; Wilkinson *et al.*, 1996; Smith, 2001; Saucède & Néraudeau, 2006).

The cassiduloid phylogenetic analysis performed by Suter (1994a) was the most complete and included all living and many fossil genera. However, possibly because of problems with character exhaustion (Wagner, 2000) and consequent high similarity among groups, Suter (1994a) ended up with many most parsimonious hypotheses to choose from and weak support for the cassiduloid families. These results led Kroh & Smith (2010) to dismember the order and propose a new classification, elevating the valid families to the status of order and removing several genera from the Cassiduloida altogether. The order Cassiduloida *sensu* Kroh & Smith (2010) consists of only three families, Cassidulidae, Neolampadidae and Pliolampadidae, but the relationships among the cassiduloids were poorly supported, and no convincing synapomorphies have been identified to support even this smaller grouping.

The composition of the family Cassidulidae (the 'true cassiduloids' because it contains *Cassidulus* Lamarck, 1801, the type genus of the order Cassiduloida) has changed considerably since Mortensen's (1948a) monograph (Table 1). Given that it retains the name of the family (and of the order Cassiduloida), *Cassidulus* is the only genus that has always been classified as a cassidulid, together with *Rhyncholampas* A. Agassiz, 1869. In addition to these taxa, > 20 other genera have been considered members of the cassidulid group at one time or another. However, most classifications (Table 1) and phylogenies published to date (Fig. 1) agree that five genera are included in this family: *Cassidulus*, *Rhyncholampas*, *Eurhodia* d'Archiac & Haime, 1853, *Glossaster* Lambert, 1918 and *Paralampas* Duncan & Sladen, 1882. Although Suter's phylogenies had good taxonomic coverage, his goal was to analyse the relationships at the order level, and few Cassidulidae were included in the analyses (Suter, 1994a, b). Therefore, delimitations of and relationships among the cassidulid genera were not robust. Also, there remains a need to explain the origin of the cassidulids in a phylogenetic framework, their diversification during the Eocene and their near-complete demise as they approached the present.

As a first step towards understanding the cassidulid's evolutionary history, our study has the following aims: (1) to propose a time-calibrated phylogenetic hypothesis of relationships among the

Table 1. Classification of the ingroup genera, selected according to previous studies and hypotheses of present study

Genera	Mortensen (1948a)*	Kier (1962)†	Mooi (1990b)	Smith & Jeffery (2000)	Kroh & Mooi (2018)	Present Study
Cassidulus	C	C	C	C	C	C
Eurhodia	C	P	C	C	C	C
Glossaster	C‡	C§	–	–	C	C
Kassandrina¶	C	–	C	–	I	I
Paralampas	C	C‖	–	Nu**	C	C
Rhyncholampas	C§	C	C	C	C	C

Footnotes include genera classified within the Cassidulidae in previous studies, and the reason why they were considered outgroups (O) or not included in the present analyses.
Abbreviations: C, family Cassidulidae; Nu, family Nucleolitidae; P; family Pliolampadidae; I, *incertae sedis*.
*Mortensen (1948a), genera with a tetrabasal apical disc: *Astrolampas* Pomel, *Fauraster* Lambert & Thiéry, *Lefortia* Cossman, *Procassidulus* (O), *Pygurostoma* Cotteau & Gauthier, *Rhynchopygus* (O) and *Vologesia* Cotteau & Gauthier. Genera lacking a complete naked zone running along the oral midline of the test: *Clypeanthus* Cotteau, *Ilarionia* Dames, *Galerolampas* Cotteau, *Gitolampas* Gauthier, *Haimea* Michelin, *Neocatopygus* Duncan & Sladen, *Oligopodia* (O), *Oligopygus* de Loriol, *Pliolampas* Pomel, *Stigmatopygus* (O), *Studeria* (O) and *Zuffardia* Checchia-Rispoli. Genera with tooth-like bourrelets: *Hypsopygaster* Bajarunas and *Australanthus* (O). Others: *Protolampas* Lambert (infraramginal periproct), *Echinanthus* Leske (*nomen dubium*), *Microlampas* Cotteau (synonym with *Echinolampas*).
†Kier (1962), genera with a tetrabasal apical disc: *Nucleopygus* Agassiz, *Ochetes* Pomel.
‡Suggested synonymy with *Procassidulus*.
§Synonym with *Cassidulus*.
¶The species *Kassandrina malayana* was previously placed in *Procassidulus* by Mortensen (1948a) and in *Cassidulus* by Mooi (1990b).
‖Suggested synonymy with *Rhynchopygus*.
**Subgenus of *Petalobrissus* Lambert.

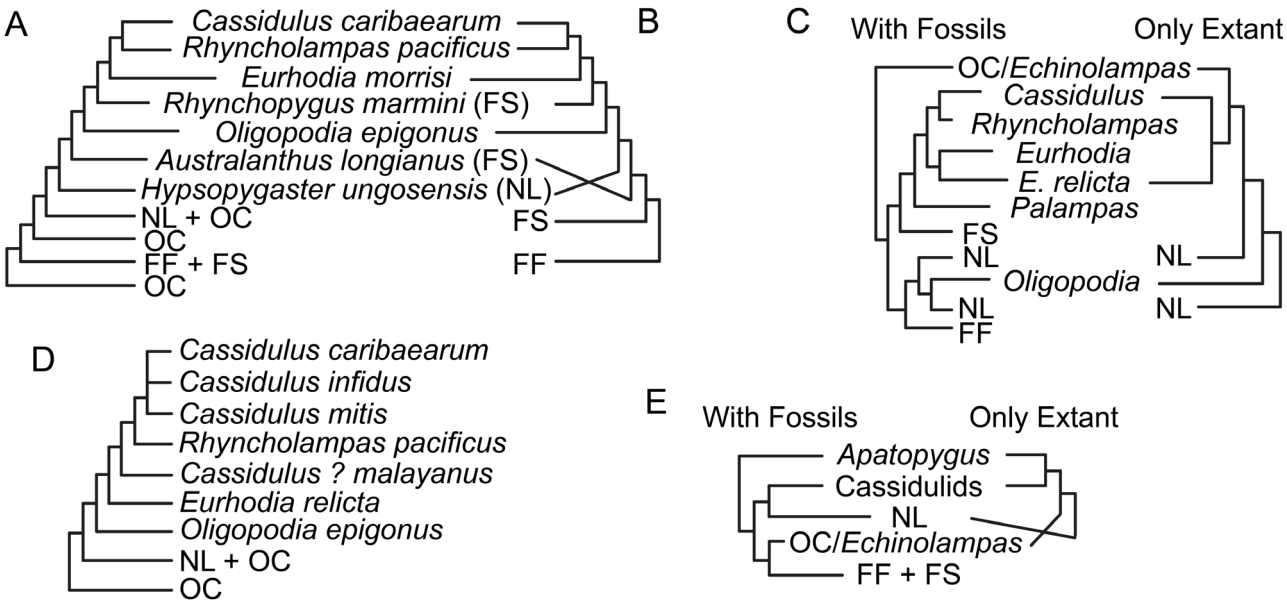

Figure 1. Previous morphology-based phylogenetic hypotheses of relationships in cassidulids and among cassidulids, faujasiids and neolampadids. A, Suter (1994a). B, Saucéde & Néraudeau (2006). C, Smith (2001). D, Suter (1994b). E, Kroh & Smith (2010). Abbreviations, following the classification of Kroh & Mooi's (2018): FF, Faujasiinae; FS, Stigmatopyginae; NL, Neolampadina; OC, other cassiduloids.

cassidulid genera and their contained species; (2) to test the taxonomic assignments to date and discuss the taxonomic implications resulting from the phylogeny; and (3) to analyse the impact of missing data and partial uncertainties in parsimony-based phylogenetic reconstruction.

MATERIAL AND METHODS

Acronyms

Advanced Light Source, Lawrence Berkeley National Laboratory, Berkeley, CA, USA (ALS-LBNL); Australian Museum, Sydney, NSW, Australia (AM); California Academy of Sciences, San Francisco, CA, USA (CAS; Invertebrate Zoology collections, CASIZ; Geology collections, CASG); Los Angeles County, Natural History Museum, Los Angeles, CA, USA (LACM; Invertebrate Zoology collections, LACM; Invertebrate Paleontology collections, LACMIP); Department of Geological and Geophysical Collections of the Mining and Geological Survey of Hungary, Budapest, Hungary (MBFSZ); Museum of Comparative Zoology, Harvard, MA, USA (MCZ); Muséum National d'Histoire Naturelle, Paris, France (MNHN); Museu Nacional, Rio de Janeiro, RJ, Brazil (MNRJ); Muzeum Przyrodnicze Uniwersytetu Wrocławskiego, Wrocław, Poland (MP MNHWU); Museum Victoria, Melbourne, Victoria, Australia (MV); Natural History Museum, London, UK (NHMUK); Naturhistorisches Museum Wien, Vienna, Austria (NHMW); Naturhistorisches Museum, Basel, Switzerland (NMB); Department of Geology and Palaeontology, Muséum d'Histoire Naturelle Genève, Switzerland (MHNG GEPI); National Museum of Natural History, Washington, DC, USA [USNM (MO and PAL)]; Swedish Museum of Natural History, Stockholm, Sweden (SMNH); University of California, Museum of Paleontology, Berkeley, CA, USA (UCMP); Florida Museum of Natural History, Gainesville, FL, USA (UF); Museu de Zoologia, Universidade Federal da Bahia, Salvador, BA, Brazil (UFBA); Echinoderm Collection, Universidade Federal de Sergipe, Itabaiana, SE, Brazil (UFISITAB); Naturalis Biodiversity Center, Leiden, The Netherlands (ZMA); Museum für Naturkunde, Berlin, Germany (ZMB); Zoological Museum, University of Copenhagen, Denmark (ZMUC); Museu de Zoologia da Universidade Estadual de Campinas, SP, Brazil (ZUEC).

Abbreviations

CI, consistency index; FAD, first appearance datum; I5, interambulacrum 5; LAD, last appearance datum; MPT, most parsimonious tree; RI, retention index; SRμCT, synchrotron radiation-based micro-computed tomography; TH, test height; TL, test length; TW, test width; Wa, adoral (opening) width; We, adoral

width; Wm, perradial zone width; Wp, petal width; Wr, poriferous zone width; Wx, ambulacral expansion (measured at the ambitus).

Numbering of plates, i.e. Arabic numerals for interambulacral plates and Roman numerals for ambulacral plates, follows Lovén's system (Lovén, 1874). Two-letter genus abbreviations were used for genus names with the same initial letter. For similar genus names, the following combinations were used: *Rhyncholampas* (*Rl.*), *Rhynchopygus* (*Rp.*), *Stigmatopygus* (*Sg.*) and *Studeria* (*Sd.*).

Taxon sampling

Ingroup taxa

Phylogenetic reconstructions of the cassiduloids (Fig. 1) have generally agreed that the monophyly of the family Cassidulidae is supported by a complete and pitted naked zone running along oral I5 and ambulacrum III. Ancestral traits that also characterize current members of this family (Kroh & Mooi, 2018) are a monobasal apical system and a marginal periproct. Over time, ≥ 30 genera have been considered members of the cassidulid group, but its classification has been unstable (see Table 1) and there is no widely accepted work of sufficiently comprehensive taxon sampling to serve as a standard for the group. Therefore, we used the traits listed above to describe the ingroup.

The type and all extant species of each genus were included in the analyses. Fossil species were included whenever well-preserved, accessible specimens were available, resulting in a total of 45 species (six extant and 39 extinct) from five genera (Table 2). Table 3 provides a summary with the taxonomic status of the species contained in each of these genera.

Genus Cassidulus: The family Cassidulidae, and concomitantly the order Cassiduloida, was based on this genus. Probably as a result of being the first genus and its broad description, > 75 cassidulid-like species (and even cassiduloid-like ones) were attributed to this genus (C. Souto, unpubl. data). The following nine species (four extant and five extinct) were included in the analyses: the type *Cassidulus caribaearum* Lamark, 1801, *Cassidulus briareus* Souto & Martins, 2018, *Cassidulus californicus* Anderson, 1905, *Cassidulus ellipticus* Kew, 1920, *Cassidulus falconensis* (Jeannet, 1928), *Cassidulus infidus* Mortensen, 1948b, *Cassidulus kieri* Adegoke, 1977, *Cassidulus mitis* Krau, 1954 and *Cassidulus trojanus* Cooke, 1942. Carter & Beisel (1987) suggested that *C. trojanus* should be transferred to the genus *Eurhodia*, but the traits they used to justify this change (i.e. deep pits in the naked zone and concave oral surface) are not present in the type species of *Eurhodia*.

Genus Eurhodia: Kier (1962) described the family Pliolampadidae and placed *Eurhodia* in it, probably owing to the presence of a longitudinally elongate peristome. However, pliolampadids do not have a naked zone in oral I5, and Mooi (1990b) reclassified *Eurhodia* in the Cassidulidae. The following 12 species (one extant and 11 extinct) were included in our analyses: the type *Eurhodia morrisi* d'Archiac & Haime, 1853, *Eurhodia australiae* (Duncan, 1877), *Eurhodia baumi* Kier, 1980, *Eurhodia calderi* d'Archiac & Haime, 1853, *Eurhodia cravenensis* (Kellum, 1926), *Eurhodia holmesi* (Twitchell in Clark & Twitchell, 1915), *Eurhodia matleyi* (Hawkins in Arnold & Clark, 1927), *Eurhodia navillei* (de Loriol, 1880), *Eurhodia patelliformis* (Bouvé, 1851), *Eurhodia relicta* Mooi, 1990a, *Eurhodia rugosa* (Ravenel, 1848) and *Eurhodia thebensis* (de Loriol, 1880). *Eurhodia relicta* is the only representative of this genus since the Late Eocene (~37.8 Mya). Mooi (1990a) placed this species in *Eurhodia* because of its resemblance to *Eu. holmesi*, although he also highlighted its great resemblance to *Oligopodia epigonus* (von Martens, 1865). Other species with questionable status are *Eu. cravenensis*, considered synonymous with *Eu. holmesi* by Cooke (1942) and Kier (1980), *Eu. calderi* and *Eu. thebensis*, considered synonymous with *Eu. navillei* by Roman & Strougo (1994). Our decision to retain all three species was based on differences noticed in our morphological analyses. For example, *Eu. cravenensis* differs from *Eu. holmesi* in having tulip-shaped anterior paired petals (vs. leaf-shaped) and six plates framing the periproct (vs. four), *Eu. thebensis* differs from *Eu. navillei* in having an elongated test (vs. oval), and *Eu. calderi* differs from *Eu. navillei* in having 12–14 pores in the anterior phyllodes (vs. seven to ten).

Genus Glossaster: This is the oldest known cassidulid genus, with the first occurrences dating back to the Campanian (~83.6 Mya, Late Cretaceous). Its fossil record indicates that this genus went extinct in the Middle Eocene (~37.8 Mya). *Glossaster* has been considered a synonym of *Procassidulus* (Mortensen, 1948a) and of *Cassidulus* (Kier, 1962), but Kier & Lawson (1978) considered *Glossaster* a genus on its own. The following three species were included in our analyses, although their classification has been unstable (see Néraudeau *et al.*, 1997; Smith & Jeffery, 2000): the type, *Glossaster sorigneti* (Michelin in Goubert, 1859), *Glossaster vasseuri* (Cotteau (1885–1889)) and *Glossaster welschi* Gauthier in Lambert, 1931.

Table 2. List of taxa included in the phylogenetic analyses and used for the phylogenetic calibration, their stratigraphic range, geographical distribution and the character coding completeness (CCC) for each species

Taxon	Estimated age (Mya)*	Reference for age assignment†,‡	Geographical distribution	CCC (%)§
Family Apatopygidae				
Apatopygus recens	0.01–0	N/A	New Zealand	100
Nucleolites scutatus	163.5–145	Kier (1962)	Western Europe	92
Order Cassiduloida				
Family Cassidulidae				
Cassidulus briareus	0.01–0	N/A	Australia	96
Cassidulus californicus	56–37.8	Squires & Demetrion (1995)	USA (CA)	83–85
Cassidulus caribaearum	0.01–0	N/A	Caribbean Sea	100
Cassidulus ellipticus	56–37.8	Squires & Demetrion (1995)	Mexico (BC) to USA (CA)	79–82
Cassidulus falconensis	[15.97–5.33]–2.58¶	Cooke (1961), Mihaljević *et al.* (2010), UCMP 123469, 123470	Venezuela	92
Cassidulus infidus	0.01–0	N/A	Brazil (BA)	100
Cassidulus kieri	66–56	Adegoke (1977)	Nigeria	94
Cassidulus mitis	0.01–0	N/A	Brazil (RJ, SP)	100
Cassidulus trojanus	37.8–33.9	Osborn *et al.* (2016)	USA (FL)	92
Eurhodia australiae	47.8–33.9	Holmes (2004)	Australia (SA)	92
Eurhodia baumi	47.8–37.8	Osborn *et al.* (2016)	USA (SC, NC)	91
Eurhodia calderi	59.2–41.2	Duncan & Sladen (1882), Afzal *et al.* (2009), UCMP 123431, 318982–318985	Pakistan	93
Eurhodia cravenensis	47.8–37.8	Kier (1980)	USA (NC)	89–90
Eurhodia holmesi	47.8–37.8	Osborn *et al.* (2016)	USA (SC, NC)	93
Eurhodia matleyi	47.8–33.9	Donovan (2004)	Jamaica	91
Eurhodia morrisi	59.2–47.8	Smith & Jeffery (2000), Afzal *et al.* (2009)	Pakistan	93
Eurhodia navillei	56–41.2	Roman & Strougo (1994), Tawadros (2012)	Egypt and Senegal	88–90
Eurhodia patelliformis	37.8–33.9	Osborn *et al.* (2016)	USA (FL)	91
Eurhodia relicta	0.01–0	N/A	Venezuela and Suriname	98
Eurhodia rugosa	47.8–37.8	Osborn *et al.* (2016)	USA (SC, NC)	94
Eurhodia thebensis	47.8–41.2	Fourtau (1913), Tawadros (2012)	Egypt	82–85
Glossaster sorigneti	47.8–41.2	Néraudeau *et al.* (1997)	France	81–82
Glossaster vasseuri	47.8–37.8	Cotteau (1885–1889)	France	92–93
Glossaster welschi	83.6–66	MNHN J00696	Algeria	74–75
Paralampas pileus	59.2–41.2	Duncan & Sladen (1882), Afzal *et al.* (2009), UCMP 318990–91	Pakistan	92–93
Paralampas rancureli	59.2–56	Smith & Jeffery (2000)	Ivory Coast	86
Rhyncholampas alabamensis	27.82–23.03	Osborn & Ciampaglio (2014)	USA (AL, MS)	90–92
Rhyncholampas anceps	56–47.8	Lambert (1933)	Madagascar	85–87
Rhyncholampas ayresi	3.6–0.01	Oyen & Portell (2002)	USA (FL)	91
Rhyncholampas carolinensis	47.8–37.8	Osborn *et al.* (2016)	USA (NC)	91
Rhyncholampas chipolana	23.03–15.97	Oyen & Portell (2002)	USA (FL)	88–89
Rhyncholampas conradi	37.8–33.9	Osborn *et al.* (2016)	USA (FL)	91
Rhyncholampas daradensis	47.8–41.2	Meunier (1906), Roman & Gorodiski (1959)	Senegal	92

Table 2. Continued

Taxon	Estimated age (Mya)*	Reference for age assignment†,‡	Geographical distribution	CCC (%)§
Rhyncholampas ericsoni	[47.8–37.8]–33.9	Osborn *et al.* (2016)	USA (FL)	88–89
Rhyncholampas evergladensis	5.33–2.58	Oyen & Portell (2002)	USA (FL)	93
Rhyncholampas globosa	47.8–33.9	Fischer (1951), UF 165741, 248491	USA (FL)	90
Rhyncholampas gouldii	33.9–23.03	Oyen & Portell (2002)	USA (FL)	92
Rhyncholampas grignonensis	47.8–37.8	Néraudeau *et al.* (1997), Carrasco (2016)	Western Europe	90
Rhyncholampas mexicana	15.97–7.25	Kew (1920), Coates (1999)	Mexico (BC)	88
Rhyncholampas pacifica	0.01–0	N/A	Mexico (BC) to Panama, Galapagos islands	100
Rhyncholampas riveroi	27.82–13.82‖	Sánchez Roig (1949)	Cuba	75–77
*Rhyncholampas rodriguezi*_A	47.8–37.8**	MNHN A22036	Cuba	87
*Rhyncholampas rodriguezi*_R	33.9–13.82**	MNHN R66851, UF 216778	Cuba	90–91
Rhyncholampas sabistonensis	47.8–37.8††	Kellum (1926)	USA (NC)	88–91
Rhyncholampas tuderi	56–37.8	Lambert (1937), MNHN A22037, A22038, R10086	Morocco	88–89
Family Neolampadidae				
Neolampas rostellata	0.01–0	N/A	Florida, Gulf of Mexico, NE Atlantic	100
Studeria recens	0.01–0	N/A	Indo-Pacific	94
Family Pliolampadidae				
Pliolampas elegantula	[23.03–]15.97–11.63[–5.33]	Kier (1962), MNHN R66890	France	93
Order Clypeasteroida				
Family Faujasiidae				
Australanthus longianus	[47.8–37.8]–33.9	Holmes (2004)	Australia (SA)	93
Faujasia apicalis	72.1–66	Agassiz & Desor (1847), Smith & Jeffery (2000)	The Netherlands and Belgium	93
Faujasia rancheriana	113–100.5	Cooke (1955)	Colombia	92
Hardouinia mortonis	72.1–66	Smith & Jeffery (2000)	USA (NC, MS, TX), Cuba	94
Hardouinia bassleri	86.3–83.6	Cooke (1953)	USA (AL)	83–84
Petalobrissus cubensis	89.8–72.1	Weisbord (1934), Cooke (1953)	Cuba, Mexico (CS), USA (TX)	94
Petalobrissus setifensis	83.6–66	Cotteau (1866), Smith & Jeffery (2000)	Algeria, Tunisia, Lybia	90–91
Procassidulus lapiscancri	72.1–66	Smith & Jeffery (2000)	The Netherlands and Belgium	93
Rhynchopygus arumaensis	83.6–72.1	Kier (1972)	Saudi Arabia	91
Rhynchopygus macari	72.1–66	Smiser (1935), Smith & Jeffery (2000)	The Netherlands and Belgium	82–84
Rhynchopygus marmini	72.1–66	Agassiz & Desor (1847), Smith & Jeffery (2000)	Western Europe	88–89
Stigmatopygus pulchellus	72.1–66	Smith & Jeffery (2000)	Oman, United Arab Emirates	90–91

Table 2. Continued

Taxon	Estimated age (Mya)*	Reference for age assignment†,‡	Geographical distribution	CCC (%)§
Order Echinolampadoida				
Family Echinolampadidae				
Echinolampas depressa	0.01–0	N/A	Colombia to USA (NC)	100
Incertae sedis and stem groups				
Kassandrina florescens	[33.9–27.82]–15.97	Souto & Martins (2018)	Australia (South)	92
Kassandrina malayana	0.01–0	N/A	Australia (WA), Indonesia	99
Oligopodia epigonus	0.01–0	N/A	Indo-Pacific	100

Type species of genera are in bold. Genera and family classification follows Kroh & Mooi (2018). Uncertain ages are given in square brackets.
*According to Cohen *et al.* (2013; updated).
†Australian formations were checked against the Australian Stratigraphic Units Database, available at http://dbforms.ga.gov.au/pls/www/geodx.strat_units.int, on 15 August 2017; and the USA formations were checked against the National Geologic Map Database, available at https://ngmdb.usgs.gov/Geolex/search, on 15 August 2017.
‡Assigning reliable ages for the Cuban specimens described by Mario Sánchez Roig is challenging. The stratigraphy of Cuban outcrops has been revised in the last 40 years, but Sánchez Roig did not provide detailed geographical and stratigraphic information about his specimens; therefore, combining the revised information with his old publications is not straightforward. Here, we assigned a broader age range for the specimens analysed, which includes Sánchez Roig's stratigraphic information and the information retrieved from the geological maps of Cuba (Academia de Ciencias de Cuba, 1988), based on the geographical information that Sánchez Roig provided.
§Lower values of completeness consider partial uncertainty as missing data.
¶Jeannet (1928) assigned *C. falconensis* to the 'serie Capadare', in the upper part of 'couches d'Ojo de Agua', Middle Miocene (serie Caparade might refer to the Capadare Formation). Cooke (1961: p. 5) mentioned that the section Jeannet (1928) called 'd'Ojo de Agua' in fact refers to two formations that range from the Middle to the Late Miocene. He also presented more information regarding the locality where the specimens were collected, Punta Gavilán; nonetheless, he also assigned *C. falconensis* to the Middle Miocene. Mihaljević *et al.* (2010) reported two records for this species: *Eurhodia falconensis*, as originally described by Jeannet (1928) placed in the original description; and *Cassidulus* (*Cassidulus*) *falconensis*, which was the classification proposed by Cooke (1961). Both records were assigned to the Middle Miocene. Lodeiros *et al.* (2013) interpreted 'Punta Gavilán' as belonging to the Punta Gavilán Formation, which is Pliocene in age. The UCMP holds specimens of *C. falconensis* from the San Gregorio Formation (Pliocene). Given that the age assignments have been challenging to interpret and the UCMP record was verified by us, we placed uncertainty in the Miocene range of the species.
‖Sánchez Roig (1949) dated *R. riveroi* to the Late Oligocene of '"las Trozas", Colonia del Central Algodones, Término Municipal de Jatibonico, Camagüey', and the geological map of Cuba indicates that the outcrops exposed in Las Trozas belong to the Guines Formation, dating from the early Middle Miocene.
**Sánchez Roig dated *R. rodriguezi* to the Early Oligocene in 1926 (original description in Sánchez Roig, 1926), but in 1952 he dated this species to the Early Miocene (Sánchez Roig, 1952). We could not locate the locality ('Cantera de las Cuevas, en el kilometro 185 del Camino de Pinar del Rio a Guane, Cuba') in the geological map of Cuba, and the specimens analysed here are from different localities; therefore, we kept the age assignment from the specimen's labels. The label of *R. rodriguezi*_A MNHN A22036 reads Middle Eocene, from Ciego de Ávila, Cuba. Ciego de Ávila is both a city and a province, which include formations from the Jurassic to the Holocene. The Middle Eocene formations in this region are the Florida Formation and the Vertientes Formation. The label of the specimen *R. rodriguezi*_R MNHN R66851 reads Miocene, from San Diego de los Banos, Pinar del Rio, Cuba. In this locality, there is an outcrop from the Early–Middle Miocene (Paso Real Formation). The specimen *R. rodriguezi*_R UF 216778 has two labels: the new label reads Early Oligocene, from Ciego de Ávila, Majagua; and the older label reads Oligo-Miocene, from Majagua, Camagüey. The outcrops exposed in the city of Majagua in the Ciego de Ávila Province date from the Late Eocene (Ferrer Formation), Oligocene, and early Middle Miocene (Arroyo Palmas Formation), with the older outcrops mostly to the north and the younger outcrops mostly to the south. Therefore, we assigned the specimen *R. rodriguezi*_R from the Oligocene to the early Middle Miocene.
††Age assignment for *R. sabistonensis* is also controversial. Cooke (1942) suggested that this species occurs at the Trent Marl (Oligocene), and specimens at UF are from the Tamiami Formation (Pliocene). Given that the identification of *Rhyncholampas* species is challenging, we decided to use the age assignment presented in the original description of the species (i.e. Castle Hayne marl, Middle Eocene).

Genus Paralampas: *Paralampas* is also an extinct cassidulid genus, with a fossil record ranging from the Maastrichtian to the Eocene (~72.1–33.9 Mya). Kier (1962) suggested that *Paralampas* could be a synonym of *Rhynchopygus*, but he was unable to analyse any specimens. Later, Smith & Jeffery (2000) considered *Paralampas* a subgenus of *Petalobrissus*, but the latter has a tetrabasal apical system and a longitudinal periproct. To our knowledge, there are seven nominal, widely distributed species of *Paralampas*. The following two species were included in our analyses: the type, *Paralampas pileus* Duncan & Sladen, 1882, and *Paralampas rancureli* Tessier & Roman, 1973.

Genus Rhyncholampas: This genus was described to include *C. caribaearum* and *Rhyncholampas pacifica* (Agassiz, 1863), because the genus *Cassidulus* was thought to be preoccupied among the Mollusca. After analysing some fossil specimens, Agassiz (1872: 153, 342) synonymized *Rhyncholampas* with *Rhynchopygus* d'Orbigny, 1856, although he was compelled to separate these genera in 1869 (Agassiz, 1869: 270). *Rhyncholampas* is the sister taxon to *Cassidulus* (Fig. 1), and some authors (e.g. Mortensen, 1948a) have considered them to be synonymous. Kier (1962: 18) mentioned that both genera include species with intermediate characteristics that make these

Table 3. Status of the known cassidulid taxa before analysis

Genus	Species analysed*	Species not analysed			Species included in phylogenetic analysis (%)
		Probably valid	Uncertain status	Misclassified	
Cassidulus	9	1	9	21	47–90
Eurhodia	12	1	12	2	48–92
Glossaster	3	1	2	0	50–75
Paralampas	2	1	2	2	40–67
Rhyncholampas	18	9	20†	0	38–67

'Species analysed' are those species where we were able to examine specimens. Of those 'species not analysed', we made taxonomic calls based on the literature: 'probably valid' are species whose morphological description and/or images most closely fit the description of their assigned genus; 'uncertain status' refers to species for which we did not have access to the literature or that had descriptions and images too poor to allow for confident identification and thus they need further morphological analysis; and 'misclassified' are species whose description and/or images clearly indicate that they should be placed in a different genus. The percentage of the species in each cassidulid genus included in the phylogenetic analysis is given in the last column: lowest value = 'species analysed'/('species analysed' + 'probably valid' + 'uncertain status'); largest value = 'species analysed'/('species analysed' + 'probably valid').

*Genus designations before the analyses. See section 'Taxonomic assignment of cassiduloids analysed in this study' for taxonomic assignments following the analyses performed here.

†Many of these described as *Pygorhynchus* Agassiz, 1839.

difficult to allocate unequivocally to either genus, leading us to analyse all available species to test the monophyly of these genera. The following 18 species (one extant and 17 extinct) currently classified as *Rhycholampas* are included in the analyses: the type, *Rl. pacifica*, *Rhyncholampas alabamensis* (Twitchell in Clark & Twitchell, 1915), *Rhyncholampas anceps* Lambert, 1933, *Rhyncholampas ayresi* Kier, 1963, *Rhyncholampas carolinensis* (Twitchell in Clark & Twitchell, 1915), *Rhyncholampas chipolana* Oyen & Portell, 1996, *Rhyncholampas conradi* (Conrad, 1850), *Rhyncholampas daradensis* (M.Lambert in Meunier, 1906), *Rhyncholampas ericsoni* (Fischer, 1951), *Rhyncholampas evergladensis* (Mansfield, 1932), *Rhyncholampas globosa* (Fischer, 1951), *Rhyncholampas gouldii* (Bouvé, 1846), *Rhyncholampas grignonensis* (Defrance, 1825), *Rhyncholampas mexicana* (Kew, 1920), *Rhyncholampas riveroi* (Sánchez Roig, 1949), *Rhyncholampas rodriguezi* Lambert & Sánchez Roig in Sánchez Roig, 1926 (its type specimen could not be analysed but two morphotypes were observed, therefore both were included in the analyses: *Rl. rodriguezi*_A has an inflated rounded test and a short petal III, whereas *Rl. rodriguezi*_R has an oval test and a relatively long petal III), *Rhyncholampas sabistonensis* (Kellum, 1926) and *Rhyncholampas tuderi* Lambert, 1937. A few *Rhyncholampas* species had already been synonymized by Cooke (1959); for example, *Rl. evergladensis* with *Rl. sabistonensis* and *Rl. alabamensis* with *Rl. gouldii* (but see Osborn & Ciampaglio, 2014, for a revalidation of *Rl. alabamensis*).

Outgroup selection

Twenty-one species, 15 extinct and six extant, were chosen as outgroup taxa (Table 2). We sampled outgroups across the various cassiduloid groups, but we gave priority to extinct species with available material in good condition, thereby avoiding the necessity of accounting for large amounts of missing data in the matrix. Also, some outgroups that diverged very early in the history of the cassiduloids, i.e. *Nucleolites scutatus* Lamarck, 1816 and *Apatopygus recens* (Milne Edwards in Cuvier, 1836), were chosen in an attempt to minimize homoplasy and problems of character exhaustion common in cassiduloids (Huelsenbeck, 1991; Wagner, 2000; Smith, 2001).

The suborder Neolampadina has been suggested as the sister group to the cassidulids (Kroh & Smith, 2010) and was represented by two extant and one extinct species: *Neolampas rostellata* Agassiz, 1869, *Pliolampas elegantula* (Cotteau, 1883) and *Studeria recens* (Agassiz, 1879). Extant Neolampadina live in deeper waters (Mooi, 1990b) and probably evolved through paedomorphosis (Philip, 1963) that resulted in poor development or even loss of petaloids.

The relationship between cassidulids and faujasiids has been controversial (Suter, 1994a; Smith, 2000; Kroh & Smith, 2010). The Faujasiidae is an extinct group, and many of its species have been classified as cassidulids at some point in their taxonomic history [e.g. *Australanthus longianus* (Gregory, 1890), *Procassidulus lapiscancri* (Leske, 1778), *Petalobrissus cubensis* (Weisbord, 1934), *Rhynchopygus marmini* (Desor in Agassiz & Desor, 1847)] and vice versa (e.g. *G. welschi*). In addition to these four faujasiid species, once classified as cassidulids, we included the following eight faujasiid outgroups in the analyses, according to availability of material: *Petalobrissus setifensis* (Coquand in Cotteau, 1866), *Rhynchopygus arumaensis* Kier, 1972, *Rhynchopygus macari* Smiser, 1935, *Stigmatopygus pulchelus* Smith, 1995,

Hardouinia mortonis (Michelin, 1850), *Hardouinia bassleri* (Twitchell in Clark & Twitchell, 1915), *Faujasia apicalis* (Desor in Agassiz & Desor, 1847) and *Faujasia rancheriana* Cooke, 1955.

We also chose two genera (*Oligopodia* Duncan, 1889 and *Kassandrina* Souto & Martins, 2018) that include extant species previously considered cassidulids and whose taxonomic status remains poorly established. *Oligopodia epigonus* was classified in the cassidulids by Mortensen (1948a) and Mooi (1990b), whereas others considered this species *incertae sedis* (e.g. Kier & Lawson, 1978). Phylogenetic hypotheses have suggested that this genus is a cassidulid (Suter, 1994a, b; Saucède & Néraudeau, 2006), but in these studies *O. epigonus* was coded as having a wide naked zone in the oral midline, an aboral hood above the periproct and a pentagonal peristome, features not present in the holotype. Smith (2001) placed *O. epigonus* in the neolampadids.

The other *incertae sedis* genus, *Kassandrina*, was recently described to include the species *Kassandrina malayana* (Mortensen, 1948b) and *Kassandrina florescens* (Gregory, 1892). Mooi (1990b) tentatively placed *K. malayana* in the genus *Cassidulus*, but this species has an aboral and longitudinal periproct rather than posterior and transverse. Owing to the presence of exclusive characteristics belonging to cassidulids (e.g. pitted naked zone) and faujasiids (e.g. basicoronal plates internally depressed), Souto & Martins (2018) decided to leave this genus unclassified rather than choosing one of these families arbitrarily. All three *incertae sedis* species mentioned here were included as outgroups in our analyses.

Finally, we included an extant Echinolampadidae, *Echinolampas depressa* (Gray, 1851), as an outgroup.

Material examined

The material is arranged in alphabetical order and using nomenclature pre-dating the analyses performed here. Abbreviations: H, holotype; N, neotype; P, paratype; S, syntype. Genus and family classification follow Kroh & Mooi (2018).

Superorder Neognathostomata Smith, 1981

Incertae sedis: Kassandrina florescens: CASG 71853; LACMIP 42070.1; MV P82080; NHMUK E3772–3773 (S). *Kassandrina malayana*: AM J.24441; ZMUC 236 (S), ZMUC 521 (S); Mortensen (1948a), Souto & Martins (2018). *Oligopodia epigonus*: CASIZ 76289, 188760; UF 2490, 4662; ZMB 1433 (H); Mortensen (1948a). *Oligopodia tapeina*: MCZ 102037 (H).

Family Apatopygidae Kier, 1962: Apatopygus recens: AM G.2029, J.7107; USNM E11084, E14626, E16325, E36767; Baker (1983). *Nucleolites scutatus*: CASG 66723, 67305, 67308, 67542; MNHN B49337 (S); USNM PAL 19546 A; Kier (1962).

Order Cassiduloida Agassiz & Desor, 1847

Family Cassidulidae Agassiz & Desor, 1847: Cassidulus briareus: MP 1267 Holotype MNHWU (H), MP 1267 Paratype MNHWU (P); Souto & Martins (2018). *Cassidulus californicus*: UCMP 11348 (N); USNM PAL 165664. *Cassidulus caribaearum*: CASIZ 112632, 112633, 112637, 112638, 112683, 222205 (N); NHMUK 87.6.27.7; USNM E13755, E36150; UF 11786–11788, 11797–11798, 11825–11826, 11892, 11933; Mortensen (1948a), Kier (1962). *Cassidulus ellipticus*: UCMP 11346 (S), 11347 (S); Squires & Demetrion (1995). *Cassidulus falconensis*: NMB M589/2 (H); UCMP 123469, 123470; USNM MO 638635, PAL 629295. *Cassidulus infidus*: SMNH-type-4859 (H); UFBA 314, 757; UFSITAB-ECH 123; Souto *et al.* (2011). *Cassidulus kieri*: USNM PAL 174760–174762 (P). *Cassidulus mitis*: CASIZ 116110; MNRJ 3673, 3674; UFBA 756; ZUEC 11, 12; Krau (1954). *Cassidulus trojanus*: CASG 74770; UF 3353, 41273, 47041, 48497, 66560; USNM MO 498996 (H). *Eurhodia australiae*: MV P146332, P146359, P146368, P317347; UCMP 318981; Duncan (1877). *Eurhodia baumi*: CASG 71844; USNM PAL 264043 (H). *Eurhodia calderi*: NHMUK EE1300 (H); UCMP 123431, 318982–318985; Duncan & Sladen (1882). *Eurhodia cravenensis*: USNM MO 353256 (H). *Eurhodia holmesi*: CASG 67852, 68450; LACMIP 14839; UCMP 123468; USNM MO 562303, PAL 264048, 264049, 264592. *Eurhodia matleyi*: NHMUK EE5193, E17666 (H); USNM PAL 444301, 461428, 706465. *Eurhodia morrisi*: CASG 33195.1; NHMUK E42344, E42345 (S), PI E741a; UCMP 318986, 318987; d'Archiac & Haime (1853), Duncan & Sladen (1882), Kier (1962). *Eurhodia navillei*: MHNG GEPI 26743 (H); MNHN R66902, R66907, R66908. *Eurhodia patelliformis*: CASG 71847; MCZ 102066 (H), 102067–102069, IPEC-3868; UF 4932, 41265; USNM MO 498988, 562299. *Eurhodia relicta*: USNM E20480 (H), E12971 (P); Mooi (1990a). *Eurhodia rugosa:* CASG 67850, 68447, 68449, 71849, 74774; UCMP 318994, 318995; USNM MO 562300 (N), 461473, PAL 264004, 264005; Kier (1962). *Eurhodia thebensis*: MNHN R62170 (S). *Glossaster sorigneti*: MNHN R62478. *Glossaster vasseuri*: MNHN J00620 (S). *Glossaster welschi*: MNHN J00696 (S). *Paralampas pileus*: UCMP 318990, 318991; Duncan & Sladen (1882). *Paralampas rancureli*: MNHN R06427 (H). *Rhyncholampas alabamensis*: USNM MO 559493 (H); Osborn & Ciampaglio (2014). *Rhyncholampas anceps*: MNHN J01155 (S). *Rhyncholampas ayresi*: UF 62977, 63062, 185774; USNM MO 648160 (H), 648161 (P), 460584. *Rhyncholampas carolinensis*: UF 230496; USNM MO

599488 (H), PAL 264052, 460867. *Rhyncholampas chipolana*: UF 66633, 215089, 215090, 235966; Oyen & Portell (1996). *Rhyncholampas conradi*: UF 117494, 278684, 278699, 278670, 278703; USNM MO 562304, PAL 460607. *Rhyncholampas daradensis* (?): MNHN R06029. *Rhyncholampas ericsoni*: UF 245016, 247899 (H), 247901, 247902 (P); USNM MO 560420, 560421 (P). *Rhyncholampas evergladensis*: UCMP 123435; UF 6069, 24524, 232256; USNM MO 371329 (P?), 371330 (P), 648147, 648148, PAL 460887, 460891, 460893, 460896; Cooke (1942). *Rhyncholampas globosa*: UF 12841, 115769, 165741, 245019, 248491 (H), 248492 (P), 252636, 252637 (P); USNM MO 562307. *Rhyncholampas gouldii*: CASG 67775, 67903; UCMP 318989, 318992, 318993; UF 5782, 67813, 156318. *Rhyncholampas grignonensis*: USNM MO 633997. *Rhyncholampas mexicana*: UCMP 11357 (H), 123471. *Rhyncholampas pacifica*: CASIZ 90704–90707, 90709, 106651, 106653; LACM E.1939-19.10, 1939-291.1; MCZ ECH-2714 (S), 2719 (S); MNHN-IE 2013-10554–2013-10556 (S); ZMB 2118; Mortensen (1948a). *Rhyncholampas riveroi*: UF 216884. *Rhyncholampas rodriguezi*: MNHN A22036 [*Rl. rodriguezi*_A]; R66851 [*Rl. rodriguezi*_R]; UF 216778 [*Rl. rodriguezi*_R]. *Rhyncholampas sabistonensis*: UF 2134; USNM MO 562301. *Rhyncholampas tuderi*: MNHN A22037, A22038, R10086 (S).

Family Neolampadidae Lambert, 1918: Neolampas rostellata: MNHN-IE-2016-897; USNM 6790, E20529, E36132; ZMA.V.ECH.5461; ZMB 5847, 7249; Döderlein (1906), Mortensen (1948a). *Studeria recens*: NHMUK 81.11.22.38 (S), 1949.2.4.61 (possibly S, previously registered as NHMUK 87.11.22.38).

Family Pliolampadidae Kier, 1962: Pliolampas elegantula: MNHN R66890.

Order Clypeasteroida Agassiz, 1835

Family Faujasiidae Lambert, 1905: Australanthus longianus: MV P19225, 19229, 20197, 146451–146462, 146827; NHMUK E42428 (S); UCMP 318988; USNM PAL 96252, 460548. *Faujasia apicalis*: CASG 74765, 74766; USNM PAL 131272, 460541; ZMA.ECH.E.7970. *Faujasia rancheriana*: UCMP 31218, 31219 (P). *Hardouinia mortonis*: CASG 74762, 74763; UCMP 123467; USNM PAL 464507, 464517, 464521, 464528. *Hardouinia bassleri*: USNM PAL 464461, 479787, 479788. *Petalobrissus cubensis*: CASG 74776; USNM PAL 131265, 131265 A. *Petalobrissus setifensis*: MBFSZ Ech 2018.1.5.1–2018.1.5.5 (from Coquand collection; therefore, holotype is possibly among them), USNM PAL 131261; Kier (1962). *Procassidulus lapiscancri*: UCMP 123466; USNM PAL 131260, 131263, 460563, 460564; ZMA.ECH.E.8178, 8180, 8184, 8185, 8874. *Rhynchopygus arumaensis*: USNM PAL 170452 (H), 170453 (P). *Rhynchopygus macari*: USNM PAL 461190. *Rhynchopygus marmini*: USNM PAL 131267. *Stigmatopygus pulchellus*: NHMUK EE4314 (H) and EE4314 (P); NHMW 2015/0525/0001, 2015/0525/0002.

Order Echinolampadoida Kroh & Smith, 2010

Family Echinolampadidae Gray, 1851: Echinolampas depressa: CASIZ 174963; NHMUK 1892.2.25.23; USNM E15144, E15565, E28085, E29737, E32973, E41070; UF 1246, 9027.

DATA COLLECTION, CHARACTERS AND CODING

Data were collected from direct observation of specimens and from the literature. Morphological analyses were performed using a stereo microscope attached to a camera lucida (if available during museum visits). Light application of ethanol with a paintbrush was used to highlight plate boundaries of dry specimens. When authorized by museum curators, fossils were cleaned and polished to reveal plate boundaries and ambulacral pores. Test measurements were taken with digital callipers to the nearest 0.01 mm. Selected drawings were digitized and converted to high-resolution images in Adobe Illustrator CS6 using a Wacom Intuos tablet.

Tube foot ossicles, pedicellariae and sphaeridia were removed with thin needles, cleaned and disarticulated using household bleach (~5% sodium hypochlorite solution) for 3–5 min, washed using three changes of distilled water and kept in absolute ethanol. They were then placed on metal stubs with double-sided carbon tape using a dropper, separated from each other using a thin needle, set aside to air-dry and imaged with a Hitachi TM-1000 SEM (Electron Microscope Laboratory, University of California, Berkeley, CA, USA). The plate patterns of the living taxa were visualized using SRμCT images obtained at the ALS-LBNL (beamline 8.3.2), following the protocol described by Souto & Martins (2018).

We selected 98 morphological features based on test shape (11 characters, 25 states), apical system (seven characters, 15 states), aboral ambulacra (20 characters, 54 states), periproct and I5 (19 characters, 54 states), peristome and basicoronal plates (20 characters, 43 states), oral ambulacra and sphaeridia (15 characters, 38 states) and tuberculation and pedicellariae (six characters, 13 states). We did not exclude any character that had high homoplasy indices in previous studies, but characters related to the internal organs were not included, because they are available for only a small subset of the extant species included here. Quantitative character states were defined based on natural, non-overlapping and obvious gaps observed

during analysis of a broad spectrum of the taxa involved in the study. Whenever ratios or quantitative measures are presented, these are merely to help delimit parameters for the character states, so that additional taxa can be coded by future workers. Only the largest specimens of each species were measured to reduce biases related to ontogenetic changes. Sixty-four characters were binary and 34 multi-state, with a total of 98 characters and 242 character states. Four quantitative characters were ordered.

The following list applies to all phylogenetic analyses (see explanation in 'Phylogenetic analyses'). Ordered characters and characters excluded from analysis 2 (A2; i.e. characters with high percentages of missing data) are indicated.

A) Test shape: aboral view.

1. Test outline: subquadrate (Fig. 2A) or rounded (Fig. 2B) (TW > 0.90 TL) [0]; oval (TW 0.75–0.90 TL; Fig. 2C, D) [1]; elongate (TW < 0.75 TL; Fig. 2E) [2]. This character codes for the relationship between the test width and the test length.
2. Test edge in aboral view: uniform, nearly straight edges (Fig. 2A, E) [0]; curved, greatest in the middle or posteriorly (Fig. 2B–D) [1]. This character codes for the shape of the ambital plates at interambulacra 1 and 4.
3. Test funnelled posteriorly: no [0]; yes (Fig. 2D, E) [1]. In tests with a funnelled posterior region, the plates in interambulacra 1 and 4 are nearly straight, and the width of the test decreases rapidly from widest point to the posterior region.

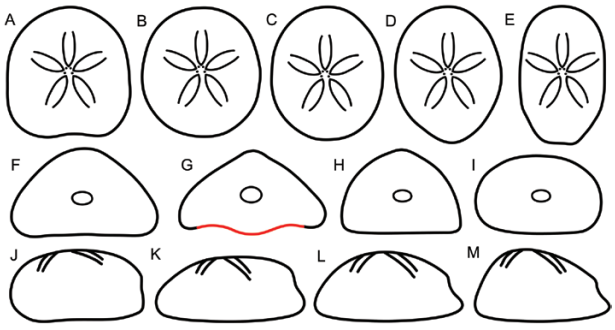

Figure 2. Outline drawings of cassiduloid tests depicting differences in shape (characters 1–9). A–E, aboral view: subquadrate (A), rounded (B), oval (C, D) and elongate (E) outline. F–I, posterior view showing transverse cross-section of test: triangular (F, G; red outline in G highlights 'M-shaped' bipartite channel) and dome-shaped (H, I). J–M, side view: outline mostly flat throughout (J), flat posteriorly (K) and with slight (L) and sharp (M) aboral slope.

B) Test shape: frontal and posterior view.

4. Shape of the transverse cross-section of the test: triangular (Fig. 2F, G) [0]; dome-shaped (Fig. 2H, I) [1]. Triangular tests are slightly inflated, and they increase in height while they diminish in width; domed tests are strongly inflated, and they increase in height while they largely maintain their width.
5. Acute peak at the apical system: absent (Fig. 2F, I) [0]; present (Fig. 2G, H) [1]. This character codes for an elevation at the apical system common in *Rhyncholampas* species and is independent from the transverse cross-section of the test. For instance, *Rl. ericsoni* has a domed test and an acute peak at the apical system.
6. Position of ambitus: low (Fig. 2F–H) [0]; high (Fig. 2I) [1]. In tests with low ambitus, the widest region is in the oral-most one-third of the test, and the ambitus is at an acute angle; in tests with high ambitus, the widest region is near or at the middle of the test, and the ambitus is at an obtuse angle.
7. Oral posterior I5 plates convex: no [0]; yes [1]. Some cassiduloids have a curvature on the oral posterior I5 plates resulting in an interradial region projected downwards. In addition, there is a depression on the plates at the oral ambulacra 1 and 5, and instead of having an open midline throughout the test, these species have an 'M-shaped' bipartite channel (Fig. 2G). This condition is clearest in *Hardouinia* but is also present in other genera.

C) Test shape: lateral view.

8. Convexity of aboral region: aboral region flat (Fig. 2J, K) [0]; slight posterior slope (Fig. 2L) [1]; steep posterior slope (Fig. 2M) [2]. Tests with a flat aboral region have a roughly uniform height from the apical system to the periproct. In tests with a posterior slope, the test decreases in height towards the periproct, meaning that the greatest centre of mass is in the anteriormost region of the test; the decrease may be slight or steep.
9. Posterior region of test truncated: no (Fig. 2K–M) [0]; yes (Fig. 2J) [1].

D) Test shape: oral view.

10. Concavity of oral region: nearly flat [0]; concavity only near the peristome [1]; concavity starting at test edge [2].
11. Inflation of posterior interambulacra: no [0]; yes [1]. This character codes for the presence of

a swollen region in the oral interambulacra 1, 4 and 5, found in *Ne. rostellata* and *Sd. recens*.

E) Apical system.

12. Apical system monobasal in adults: no [0]; yes [1]. The apical system in *Ap. recens* is tetrabasal in juveniles and monobasal in adults, possibly because of the fusion of the genital plates. Given that we do not have information about the ontogenetic changes in most fossil taxa, we chose to code this character for adults only.
13. Length of apical system in relationship to the test length: large (> 8.5% of TL) [0]; medium-sized (6.5–8.5% of TL) [1]; small (< 6.5% of TL) [2]. Measurements of the apical system were taken from the anterior margin of ocular plate III to the posteriormost region of the apical system (posterior edge of madreporic plate or of ocular plates I and V). Only mature specimens (i.e. with all gonopores well developed) were measured. For species with strong sexual dimorphism in gonopore size (e.g. *Sd. recens*), only males were measured.
14. Number of gonopores: four [0]; three [1].
15. Symmetry among gonopores: symmetric [0]; asymmetric [1]. Gonopores are asymmetric when gonopores 1 and 2 are displaced adorally and aborally, respectively, meaning that the position of the gonopores in the left and right side of the apical system is asymmetric. For species with three gonopores, symmetry was based on the position of the posterior gonopores in relationship to the centre of the apical system.
16. Location of ocular plates: between gonopores [0]; beyond gonopores [1]. In species with strong sexual dimorphism in gonopore size (e.g. *Sd. recens*), the ocular plates are located beyond the gonopores in males, and beyond the gonopores or between their adoral edge in females. We coded for the condition in males.
17. Madreporic plate extended posteriorly: no [0]; yes [1]. In some species, the posterior region of the madreporic plate has an acute rather than a curved or flat edge, ending beyond gonopores 1 and 4.
18. Hydropores: abundant, all over madreporic plate [0]; few (≤ 15), confined to a small region in madreporic plate [1].

F) Aboral ambulacra.

Neolampas rostellata does not have developed petals, and their ambulacral system is reduced to single and rudimentary pores, except for the phyllodes, which are well developed. Characters 19–26, 28–30 and 32 code for features of the aboral ambulacra not applicable to this species.

19. Longest petal: I and III roughly the same size [0]; petal I longest [1]; petal III longest [2]. In species with unequal columns of pore-pairs, we measured the longest column.
20. Posterior paired petals short: no [0]; yes [1]. Petals I and V were considered short when their length was < 90% the length of the anterior paired petals.

G) Aboral ambulacra: petal III.

21. Petal III, adoral shape (Fig. 3A): wide (Wa/Wm > 0.70) [0]; convergent (Wa/Wm = 0.40–0.70) [1]; tapering (Wa/Wm < 0.40) [2]. The ancestral state is a divergent petal, in which the pores at the end of the petal follow the growth in plate width and become more separated; in contrast, in tapering petals, the pores at the end of the petal are often positioned slightly closer to the midline of the petal.
22. Petal III, shape of columns of respiratory podia: both straight (Fig. 3B, C) [0]; inner straight and outer bowed (Fig. 3D) [1]; both bowed (Fig. 3E, F) [2]. This character codes for the change in width of the plates in the petal: some have constant width throughout; others increase and then decrease in width.
23. Petal III, width of poriferous zone in relationship to interporiferous zone (Fig. 3A): very wide (Wr > Wm) [0]; wide (Wm ≥ Wr and Wm < 2Wr) [1]; narrow (Wm > 2Wr) [2]. This character codes for the relationship between the region of the petal responsible for gas exchange (poriferous) and the region with more primary spine coverage (interporiferous). In some species, the region for gas exchange is very reduced and the area with primary spines is large; in others, the region for gas exchange takes up most of the petal area.
24. Petal III, length of a and b columns of respiratory podia: equal or differ by one pore-pair (Fig. 3A) [0]; differ by more than one pore-pair [1].

H) Aboral ambulacra: petals II and IV.

25. Shape of anterior paired petals: straight (Fig. 3B) [0]; V-shaped (Fig. 3C) [1]; oval (Fig. 3D) [2]; tulip-shaped (Fig. 3E) [3]; leaf-shaped (Fig. 3F) [4]. These states are usually distinguished by the width of the ambulacral plates throughout the petal length and by the position of the inner pores. In straight petals,

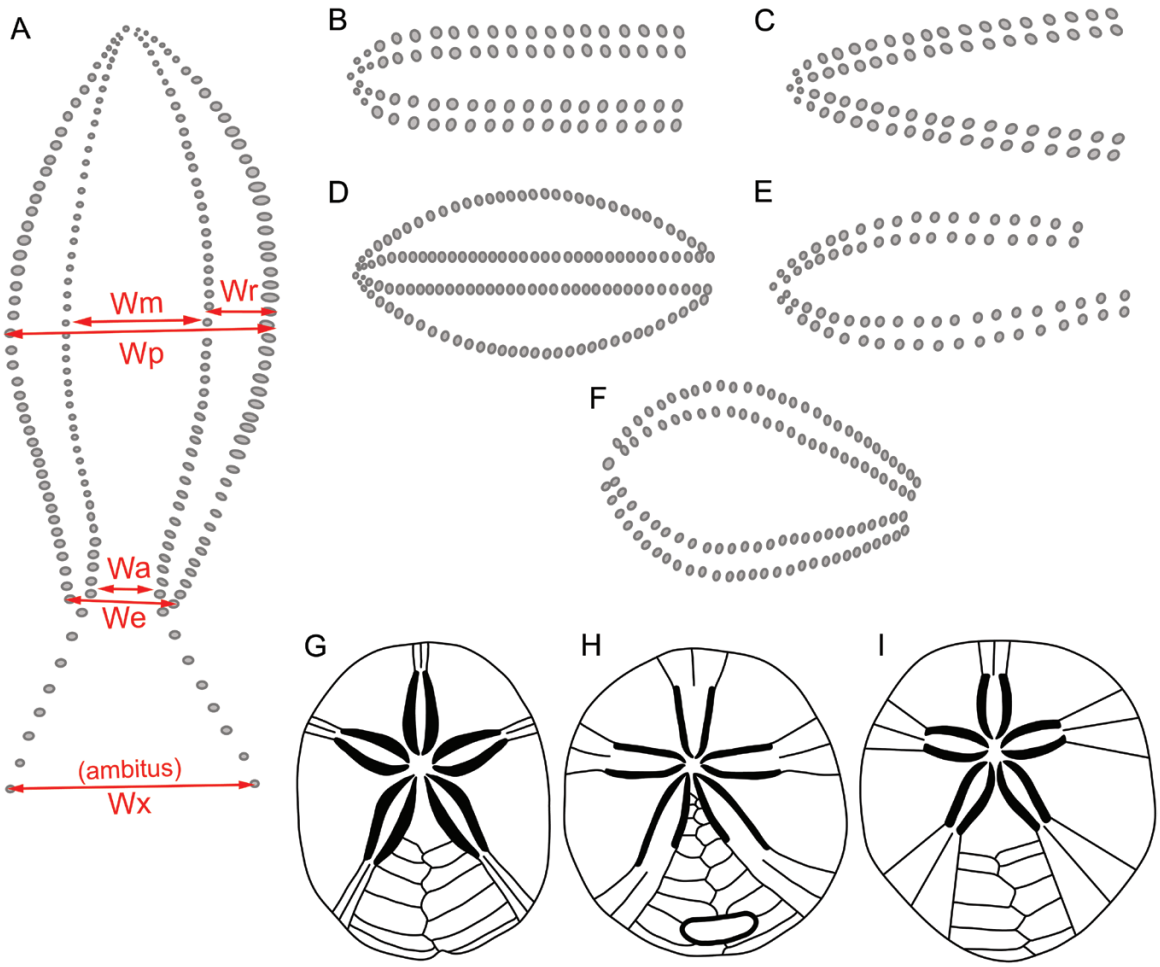

Figure 3. A, drawings of a petal showing measurements for characters 21, 23, 28, 34 and 36. Abbreviations: Wa, adoral (opening) width; We, adoral width; Wm, perradial zone width; Wp, petal width; Wr, poriferous zone width; Wx, ambulacral expansion (measured at the ambitus). B–F, drawings showing character states for petal shape (character 25) defined as straight (B), V-shaped (C), oval (D), tulip-shaped (E) and leaf-shaped (F). G–I, outline drawings of tests showing different ambulacral expansion types: uniform (G), slight (H) and strong (I). Images refer to characters 21–28 and 34–36.

the ambulacral plates have roughly the same width, and the columns of respiratory podia are straight and parallel. In the other petal shapes, the ambulacral plates increase in width towards the middle of the petal. This increase may be continuous throughout the petal, while the inner column is straight but not parallel, resulting in V-shaped petals; or the ambulacral plates decrease in width from the middle to the end of the petal, resulting in a bowed outer column of respiratory podia. In the presence of bowed outer columns, straight and parallel inner columns result in oval petals, bowed and open (i.e. broadly separated) inner columns result in tulip-shaped petals, and bowed and tapering (i.e. end of petal is nearly closed) inner columns result in leaf-shaped petals.

26. Length of a and b columns of respiratory podia, paired anterior petals: equal or differ by one pore-pair (Fig. 3B–D, F) [0]; differ by two to four pore-pairs (Fig. 3E) [1]; differ by five or more pore-pairs [2].

I) Aboral ambulacra: petals I and V.

27. Shape of the ambulacra at paired posterior petals: uniform (Fig. 3H) [0]; bowed (Fig. 3G, I) [1]. The shape was evaluated based on the difference between the widest region of the petal and the width of the plates at the end of the petal. In bowed petals, the width of the plates increases up to the middle of the petal and then decreases by > 25% towards the end.
28. Width of a and b columns of respiratory podia (Wr in Fig. 3A) at paired posterior petals: same

width [0]; width of inner column < 80% width of outer column [1]. The a and b columns of respiratory podia are usually symmetric, but in a few cases, columns 1b and 5a are wider than 1a and 5b.

29. Length of a and b columns of respiratory podia at paired posterior petals: equal or differ by one pore-pair [0]; unequal and differ by more than one pore-pair [1]. Most cassiduloids have columns of pore-pairs of the same size, but in a few species the number of pore-pairs may vary significantly between individuals of the same species (i.e. *Rl. pacifica*, whose columns may differ by three to seven pore-pairs). This condition appears early in the life of the echinoid because of different timing in the development of both columns and, therefore, should not be influenced by the size of the specimen.

J) Aboral ambulacra: general characteristics of petals.

30. Shape of outer (i.e. adradial) respiratory podia in paired petals: slit-like [0]; elongated [1]; rounded [2]. In all species, the outer pores are rounded internally, but in some cases these pores expand as they approach the surface of the test, becoming elongated (width is maintained) or slit-like.
31. Density of primary tubercles in interporiferous zone: high (Fig. 4A) [0]; low (Fig. 4B, C) [1]. The density of tubercles is high when there is no space among them, and low when the mean distance among primary tubercles is greater than the diameter of a single tubercle so that additional tubercles could be accommodated among them.
32. Tuberculation of poriferous zone: miliary tubercles only [0]; miliary and one or two sparse primary tubercles [1]; miliary and three to five often reduced primary tubercles [2]; six or more reduced primary tubercles [3]. Some species have small primary tubercles in the poriferous zones; although reduced in size, these are still larger than the miliary tubercles.
33. Last inner pore of paired petals on occluded plate: no [0]; yes [1].

K) Aboral ambulacra: plates beyond posterior paired petals.

34. Expansion of the posterior ambulacra beyond petals (Fig. 3A): uniform (Fig. 3G) [0]; slight expansion (Fig. 3H) [1]; strong expansion (Fig. 3I) [2]. Expansion (Wx) was estimated in relationship to the width of the plates at the end of the posterior petals (We): slight expansion is an increase by ≤ 100%, and strong expansion is an increase of > 100%.
35. Orientation of posterior ambulacra beyond petals: curved anteriorly (Fig. 3H) [0]; straight expansion following ambulacra (Fig. 3G, I) [1].
36. Amount of expansion (Wx) in relationship to greatest width of posterior petals (Wp) (Fig. 3A): petal > 5% wider (Fig. 3G) [0]; same width (Fig. 3H) [1]; expansion > 5% wider (Fig. 3I) [2]. This ratio apparently changes with ontogeny (i.e. expansion grows faster with ontogeny); therefore, only the larger specimens of each species were analysed.
37. Shape of ambulacral plates beyond posterior petals: rectangular, wider than long [0]; squared or slightly longer than wide [1]. This character codes for the first four plates after the end of the petal. Rectangular plates are present when the ambulacrum is wide and the pores beyond petals are close to one another.
38. Placement of pores beyond posterior petals: near or at adradial suture (Fig. 4A) [0]; between adradial suture and the middle of the plate (Fig. 4B) [1]; running thorough the

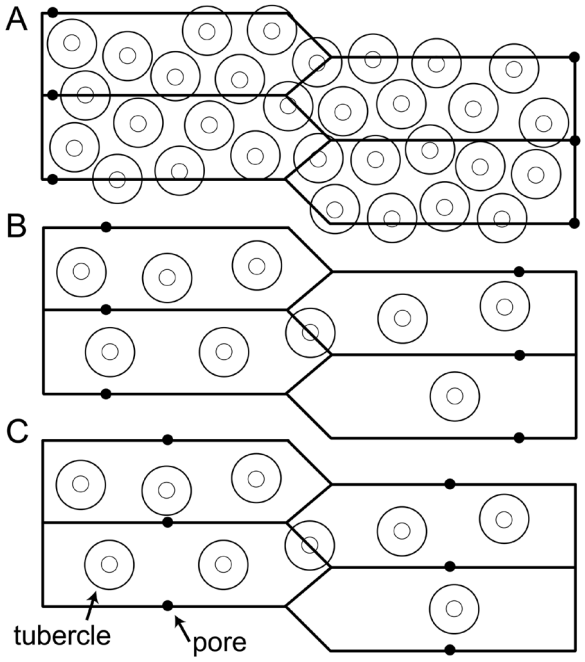

Figure 4. A–C, drawings of ambulacral plates beyond posterior petals. Black filled circles represent the pores, and concentric circles represent primary tubercles. Images refer to characters 31 and 38.

midline of the plate (Fig. 4C) [2]. For this character, we analysed the placement of the pores from the ambital plates. This character codes for the position of the pore on the outside of the test (i.e. external view). Given that the pores may not follow a straight path across the stereom (i.e. through the test wall), their position from the inside of the test side may differ.

L) Periproct and interambulacrum 5.

39. Periproct position: aboral [0]; marginal [1]; oral [2].
40. Presence of a prominent aboral hood over periproct: no (Fig. 5A, C) [0]; yes (Fig. 5B) [1]. A hood is formed when the aboral plates framing the periproct curve and extend, forming a hood that covers the periproct opening from above.
41. Shape of lateral plates framing periproct: bent inwards (Fig. 5C, E) [0]; straight (Fig. 5A, B, D) [1]. Initially, the periproct of the cassiduloids was placed in a groove formed by the bending of the lateral plates framing it. But in many groups, the lateral plates do not bend and are narrower as a result.
42. Lateral plates framing periproct supported internally by "buttresses": no [0]; yes (Fig. 6A) [1]. The plates framing the periproct may be supported internally by an additional layer of stereom that connects them.
43. Periproct with subanal shelf: no (Fig. 5A, C) [0]; yes (Fig. 5B) [1]. A subanal shelf is formed by the inward and horizontal elongation of the adoral plates framing the periproct.
44. Periproct orientation: longitudinal (width < length) [0]; equant (width = length) [1]; transverse (width > length) [2]. The lateral plates framing transverse periprocts are usually shorter and narrower than the lateral plates framing longitudinal periprocts.
45. Periproct tear-shaped: no [0]; yes [1]. In a tear-shaped periproct, the width increases from the aboral to the oral region.
46. Plates on periproctal membrane: one row of medium-sized plates and many small plates (Fig. 6B) [0]; two rows of medium-sized plates and few small plates (Fig. 6C) [1]; one row with three large plates (Fig. 6D) [2]. Not included in A2.
47. Anus placement in peristomial membrane: in the centre (Fig. 6B) [0]; on the aboral edge (Fig. 6C, D) [1]. Not included in A2.
48. Shape of interambulacral plates beneath periproct: concave, forming a groove [0]; convex [1]. This character is inapplicable to the taxa with a periproct near or at the oral surface.
49. Minimum number of plates on I5, between the basicoronal plate and the base of the periproct (plate identity in parenthesis and referenced in Fig. 6E): ≥ 11 (5.a.11 onwards) [0]; ten (5.a.10) [1]; nine (5.a.9) [2]; eight (5.a.8) [3]; seven (5.a.7) [4]; six (5.a.6) [5]; five (5.a.5) [6]. This character codes for the position of the periproct with respect to specific plates within I5. The number of plates may undergo a slight variation within a species (usually by only one plate), but it does not vary with the size of the specimen. This number is also not related to the general size of the species; for instance, *Rl. mexicana* (TL = 70 mm) and *Eu. australiae* (TL = 26 mm) have the same number of plates. Ordered 0–1–2–3–4–5–6.
50. Minimum number of plates framing the periproct (Fig. 6F): ten or more [0]; nine [1]; eight [2]; seven [3]; six [4]; five [5]; four [6]. This character represents the sum of the number of plates framing the entire periproct (i.e. on both sides) and is not necessarily

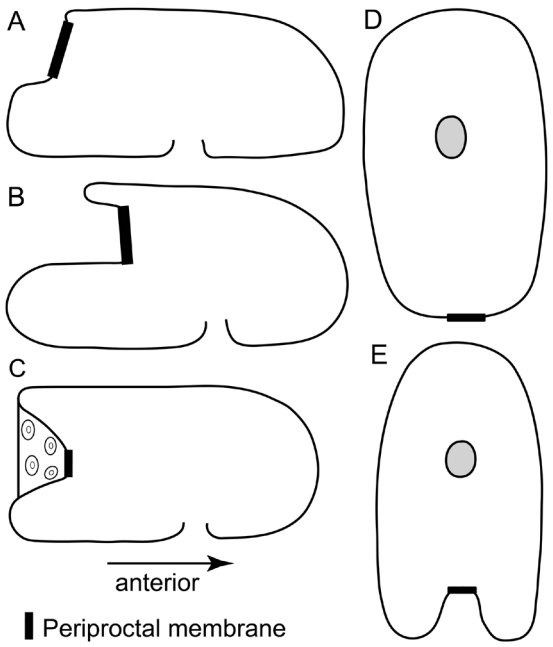

Figure 5. Outline drawings of the cross-section of the test along the anterior–posterior axis, showing the test outline in side view (A–C) and in aboral view (D, E); peristome in light grey, concentric circles represent the primary tubercles, and filled black bar represents placement of the periproctal membrane (membrane is placed inside the test in C and E because of the bending of the interambulacral plates). Images refer to characters 40, 41 and 43.

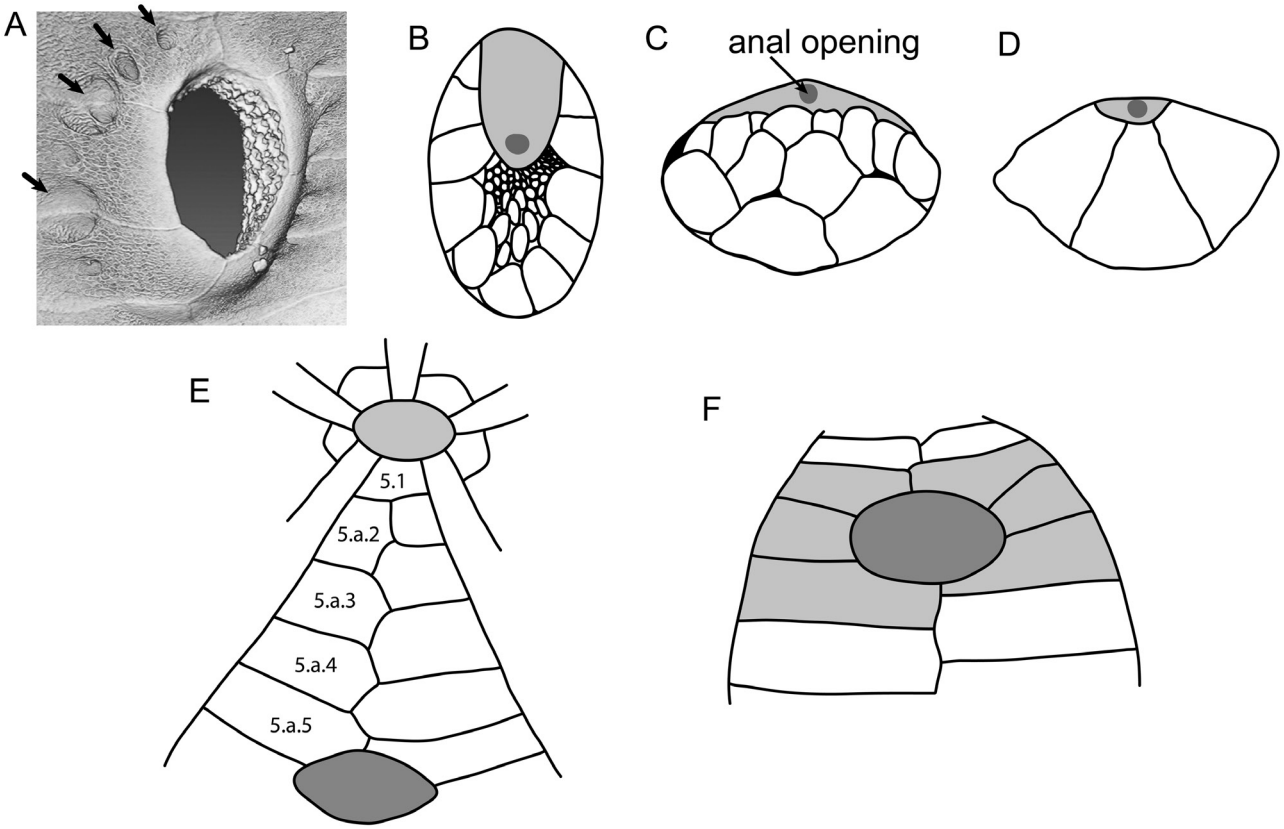

Figure 6. A, SRμCT image of the periproct of *Oligopodia epigonus* (UF 2490) in internal view, showing the periproctal "buttresses" (arrows). B–D, drawings of the different periproctal plate arrangements and placement of anal opening (periproctal membrane in light grey, anal opening in dark grey). E, drawing of the adoral region and interambulacrum 5 seen from the inside of the test (peristome in light grey and periproct in dark grey; plate identity based on the system of Lovén, 1874). F, drawing of the posterior region of the test showing, in this case, the six interambulacral plates framing the periproct in light grey (periproct in dark grey). The drawings were based on specimens as follows: B, *Apatopygus recens* USNM E36767; C, *Rhyncholampas pacifica* (CASIZ 90706); F, *Cassidulus briareus* (MP 1267 Paratype MNHWU). Modifications were made to some drawings to illustrate various character states. Images refer to characters 42, 46, 47, 49 and 50.

correlated with the size of the periproct, given that the length of the plates may vary across taxa. Ordered 0–1–2–3–4–5–6.

51. Presence of primary tubercles in posterior region of I5 basicoronal plate and adoral region of plates 5.2: absent or few [0]; abundant (more than five tubercles) [1]. Some species have tubercles near the peristome regardless of the presence (and width) of a naked zone. The tubercles may be sparse along the phyllodes or randomly distributed (variable within a species), or abundant along the phyllodes and in the middle of the plate.
52. Naked zone running along oral I5: absent (Fig. 7A) [0]; reduced (Fig. 7B) [1]; developed (Fig. 7C–E) [2]. A reduced naked zone has only a small reduction in tubercle density, and it does not reach the posterior edge of the test.
53. Width of I5 naked zone in relationship to the test width: narrow (< 10% TW; Fig. 7C, D) [0]; wide (≥ 12% TW; Fig. 7E) [1]. This character was coded based on the broadest region of the naked zone, usually in the middle.
54. I5 granular: no [0]; yes [1]. Although the naked zone is free of primary spines, miliary spines are still present. In some species, there is an increased density of miliary tubercles, giving a granular appearance.
55. Pits on I5: absent [0]; finely pitted [1]; deeply pitted [2]. The distribution of pits in the naked zone was very variable. Therefore, we coded only for their size rather than their distribution.
56. Pits on aboral edge of interambulacral basicoronal plates: absent [0]; present (Fig. 8E) [1]. Pits may be large and deep (as in

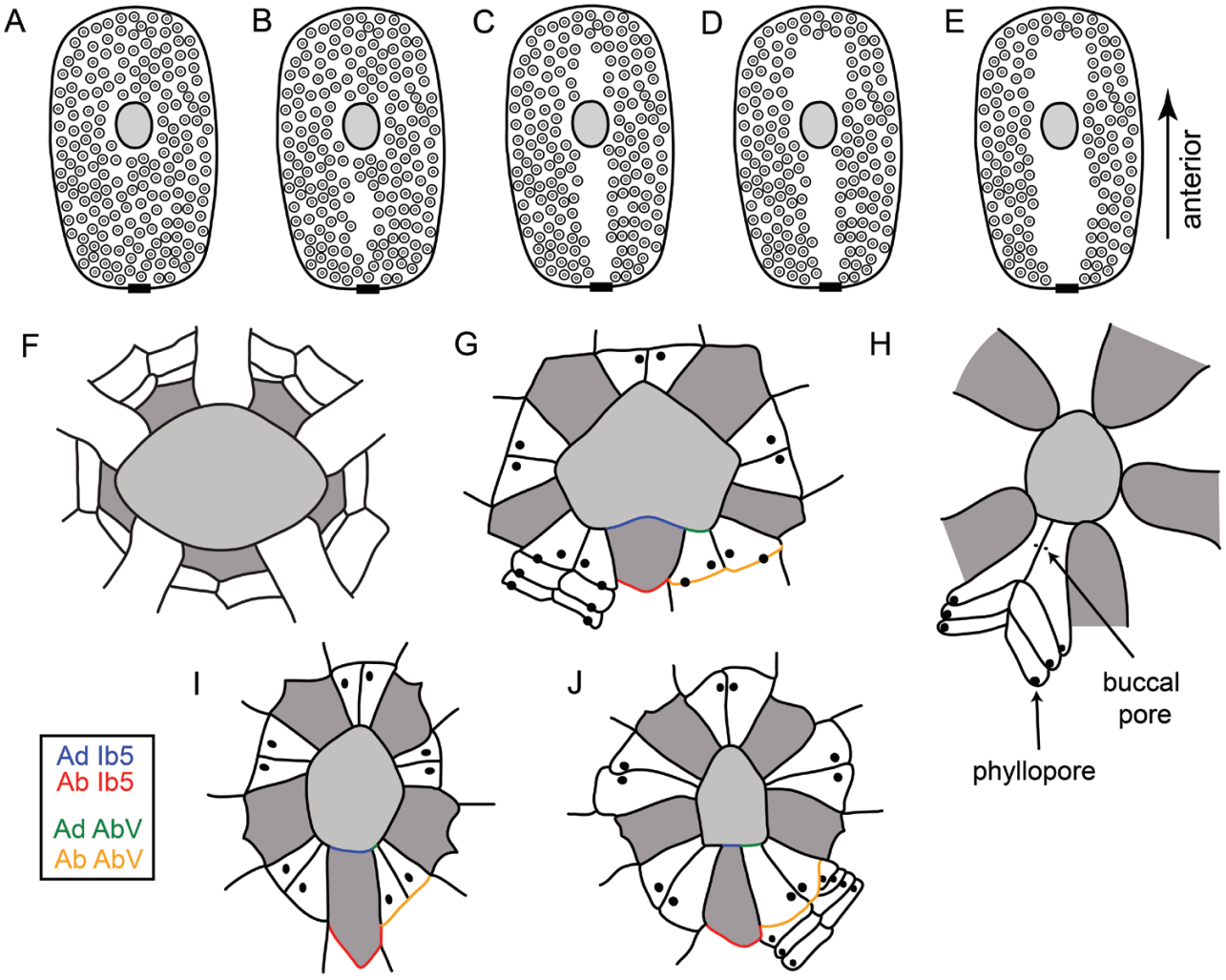

Figure 7. A–E, drawings of the oral region of the test, showing different patterns of tuberculation (concentric circles represent primary tubercles). F–J, drawings of the adoral region of the test seen from the outside. Black bar represents the periproct; peristomial membrane in light grey, interambulacral basicoronal plates in dark grey, aboral edge of interambulacral basicoronal plate 5 ('Ab Ib5') in red, adoral edge of interambulacral basicoronal plate 5 ('Ad Ib5') in blue, aboral edge of ambulacral basicoronal plate V ('Ab AbV') in orange, and adoral edge of ambulacral basicoronal plate V ('Ad AbV') in green. Drawings F–J were based on: F, *Echinolampas depressa* (USNM E32973); G, *Cassidulus mitis* (ZUEC 11); H, *Faujasia apicalis* (USNM PAL 131272); I, *Eurhodia holmesi* (USNM 264592); and J, *Hardouinia bassleri* (USNM PAL 464461). Modifications were made to some drawings to illustrate various character states. Images refer to characters 52, 53, 57, 59, 63, 67–71, 75 and 77.

some *Eurhodia*) or small and shallow (as in *Au. longianus*).

57. Naked zone running along oral ambulacrum III: absent (Fig. 7A, B) [0]; narrow (Fig. 7C) [1]; wide (Fig. 7D, E) [2]. The width of the naked zone in ambulacrum III was estimated based on the naked zone in I5. Naked zone III is usually larger, but in some species it is narrower than the naked zone in I5. If the naked zone was equally narrow or equally wide throughout, species were coded as having a narrow or wide naked zone III, respectively.

M) Peristome and basicoronal plates.

58. Peristome orientation: transverse (width > 1.1 times length) [0]; equant (width = 0.9–1.1 times length) [1]; longitudinal (width < 0.9 times length) [2].
59. Shape of peristome: (sub)pentagonal (Fig. 7G–J) [0]; oval (Fig. 7A–F) [1]. The peristome in some cassiduloids (i.e. *C. infidus*) develops

from a circular to a pentagonal shape, passing through a subpentagonal stage when juvenile.

60. Peristome position: near the centre or slightly anterior [0]; very anterior [1]. Peristomes were considered very anterior when their posterior edge was < 42% of the TL from the anterior ambitus.
61. Accretion of stereom on interambulacral basicoronal plates: absent or low (Fig. 8A, C) [0]; high (Fig. 8B, D) [1]. In some species, there is accretion of a thick stereom layer on the basicoronal plates, forming solid bourrelets.
62. Deep depression on interambulacral basicoronal plates: absent (Fig. 8B, D) [0]; present (Fig. 8A, C) [1].
63. Bourrelet 5 bulged anteriorly: no (Fig. 7F, H–J) [0]; yes (Fig. 7G) [1]. In some species, the posterior region of the peristome is strongly convex adorally; in others, this anterior projection is weak or absent, resulting in a nearly flat posterior edge.
64. Bourrelets pointed: no [0]; yes (Fig. 8E) [1]. Developed bourrelets are usually smoothly bulged, but sometimes they project outwards (towards the sediment), forming a pointed tip.
65. Bourrelets tooth-like: no [0]; yes (Fig. 8F) [1]. In tooth-like bourrelets, the sides are straight instead of rounded, and the aboral region of the bourrelet is wider than the adoral region.
66. Bourrelet 5 poorly developed: no [0]; yes [1]. This character codes for the development of bourrelet 5 in relationship to bourrelets 2 and 3. Despite being undeveloped, bourrelet 5 may still be slightly bulged, pointed or tooth-like.
67. Basicoronal plates 1 and 4 narrower than basicoronal plate 5: no (Fig. 7I, J) [0]; yes (Fig. 7G) [1].

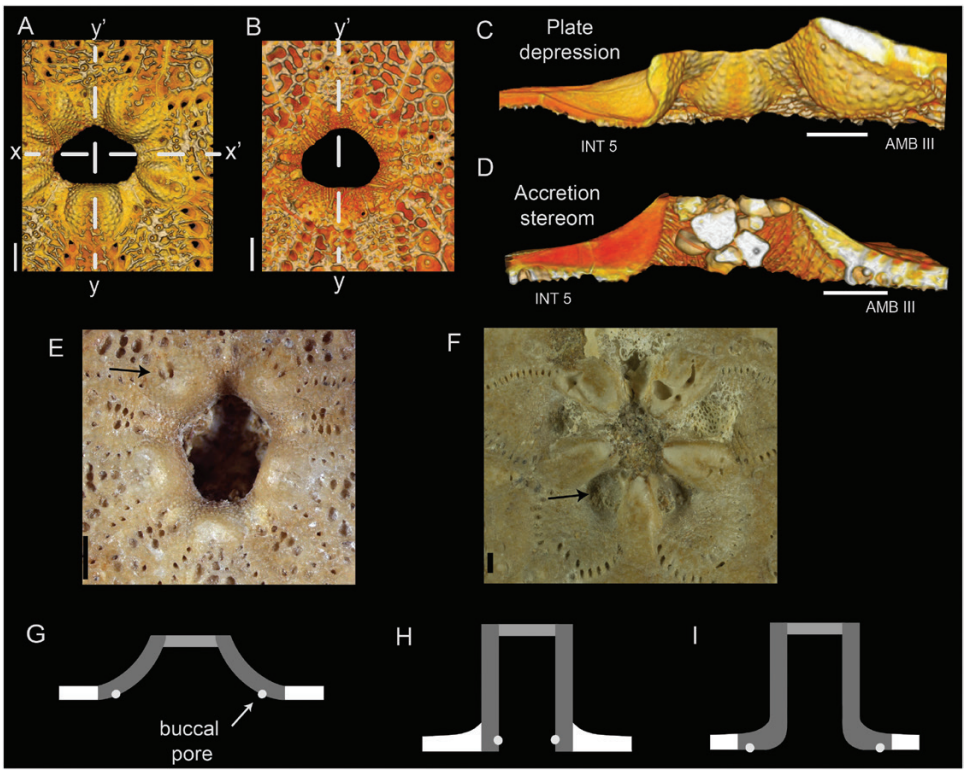

Figure 8. A–D, SRμCT-based volume renderings of bourrelets from *Kassandrina malayana* (ZMUC 236; A, C) and *Cassidulus briareus* (MP 1267 MNHWU; B, D). A, B, oral view of test showing the peristome and part of the phyllodes I and III–V; vertical dotted lines indicate region depicted in C, D, i.e. cross-section *y–y′* axis of bourrelet 5 on the left, and of phyllode III on the right (the inside of the test is towards the top of the page) (modified from Souto & Martins, 2018: fig. 10). E, F, images of the adoral region of *Eurhodia australiae* (UCMP 318981; E) (arrow indicates pits in bourrelet 2) and of *Hardouinia mortonis* (UCMP 123467; F) (arrow indicates adoral depression in ambulacral basicoronal plate I). G–I, drawings of the adoral region of the test in cross-section (cross-section plane indicated by the *x–x′ axis in A). Peristomial membrane in light grey, interambulacral basicoronal plates in dark grey, and post-basicoronal interambulacral plates in white. Abbreviations: AMB, ambulacrum; INT, interambulacrum. Images refer to characters 56, 61, 62, 64, 65, 72 and 73. Scale bars: 1 mm (A, B, E); 2 mm (F).*

68. Oral surface of I5 basicoronal plate longer than wide: no, wider or equant (Fig. 7F, G) [0]; yes (Fig. 7I, J) [1].
69. Aboral edge of I5 basicoronal plate expands beyond aboral edge of ambulacrum V basicoronal plate: no (Fig. 7G) [0]; yes (Fig. 7I, J) [1].
70. Adoral edge of I5 basicoronal plate more than twice as wide as adjacent ambulacrum V basicoronal plate: yes (Fig. 7G, I) [0]; no (Fig. 7J) [1].
71. Size of basicoronal plates I and V along the perradial suture: short [0]; medium-sized [1]; enlarged [2]. The size was estimated based on the orientation and size of the second ambulacral plate. When the basicoronal is short, the second plate is diagonal to the midline of the phyllode (Fig. 7H). When it is medium-sized, the second plate is perpendicular to the midline of the phyllode (Fig. 7G), and when it is enlarged, the second plate is a demiplate (Fig. 7J).
72. Shape of ambulacral basicoronal plates: flush or wall-like [0]; bent [1]. The shape of the plates apparently influences where the first pores are located: flush basicoronal plates are slightly curved, and the first pores sometimes start deep inside the peristome (Fig. 8G); wall-like basicoronal plates are straight, and the first pores are placed at the adoral region of the plate, often facing the inside of the peristome (Fig. 8H); and in bent plates, a high proportion of the plate is on the adoral side, and the first pores are located close to the phyllodes, facing outwards (Fig. 8I).
73. Adoral region of ambulacral basicoronal plate depressed: no [0]; yes (Fig. 8F) [1]. Depressed plates are often enlarged aborally, and their lowest region is usually lower than the peristomial opening.
74. Ambulacral basicoronal plates with more than two pores: no [0]; yes [1].
75. First pore in ambulacral basicoronal plate modified into a buccal pore: no (Fig. 9D) [0]; reduced (Figs. 7H, 9E) [1]; distinct (Figs. 7G, I, J, 9A–C, F) [2].
76. Distance between first and second ambulacral pores: near (Fig. 9A–D, F) [0]; far (Fig. 9E) [1]. When the pores are far from each other, there is a large and noticeable gap between them.
77. Placement of second ambulacral pore: in the middle of the plate, often aborally (Fig. 7G) [0]; aborally and near the adradial suture (Fig. 7H) [1]. One plate on each pair of ambulacral basicoronal plates in cassiduloids has at least two pores. In species with only two pores, the second pore is always placed aborally, but in species with more than two pores, the placement of the pores along the anterior–posterior axis will vary according to the number of pores present.

N) Oral ambulacra: phyllode III.

78. Shape of outer column of anterior phyllode: straight (Fig. 9A, D) [0]; barrel-shaped (Fig. 9B) [1]; triangular (Fig. 9C, E, F) [2]. Straight phyllodes have parallel columns of pores; barrel-shaped phyllodes have their greatest width in the middle; and triangular phyllodes have their greatest width adorally.

O) Oral ambulacra: phyllodes II and IV.

79. Arrangement of columns of paired anterior phyllodes: one column (inner column absent; Fig. 9A, E) [0]; one column and scattered pores (Fig. 9C, F) [1]; two complete columns (inner column throughout phyllode; Fig. 9B, D) [2]. In phyllodes in which the inner column is complete, the outer column is usually composed only of demiplates.
80. Shape of outer column of paired anterior phyllodes: rows of three (Fig. 9D) [0]; straight or barrel-shaped (Fig. 9A–C, F) [1]; tapering (Fig. 9E) [2]. In tapering phyllodes, the first phyllopores are widely separated while the last phyllopores are very close to each other.
81. Maximal number of primary plates in paired anterior phyllodes: ≥ 11 [0]; eight to ten [1]; five to seven [2]; up to four [3]. Character states were chosen based on intraspecific variability. For example, some species had specimens with five to seven or eight to ten pores but never outside of these ranges. Ordered 0–1–2–3.

P) Oral ambulacra: phyllodes I and V.

82. Size of posterior phyllodes: long, last phyllopore aboral to second interambulacral plate [0]; short, last phyllopore adoral to third interambulacral plate [1].
83. Maximal number of primary plates in posterior phyllodes: ≥ 12 [0]; eight to 11 [1]; four to seven [2]. Character states were chosen based on intraspecific variability. Also, in phyllodes with up to seven pores the pores are spaced out, but in phyllodes with ≥ 12 pores the pores are close together and the phyllode is highly developed. Ordered 0–1–2.
84. Arrangement of outer phyllopores in external view: pores in a uniform column (Fig. 9A–E) [0]; pores scattered (Fig. 9F) [1]. Phyllopores are usually placed near the adradial suture, but in some species the phyllopores are also

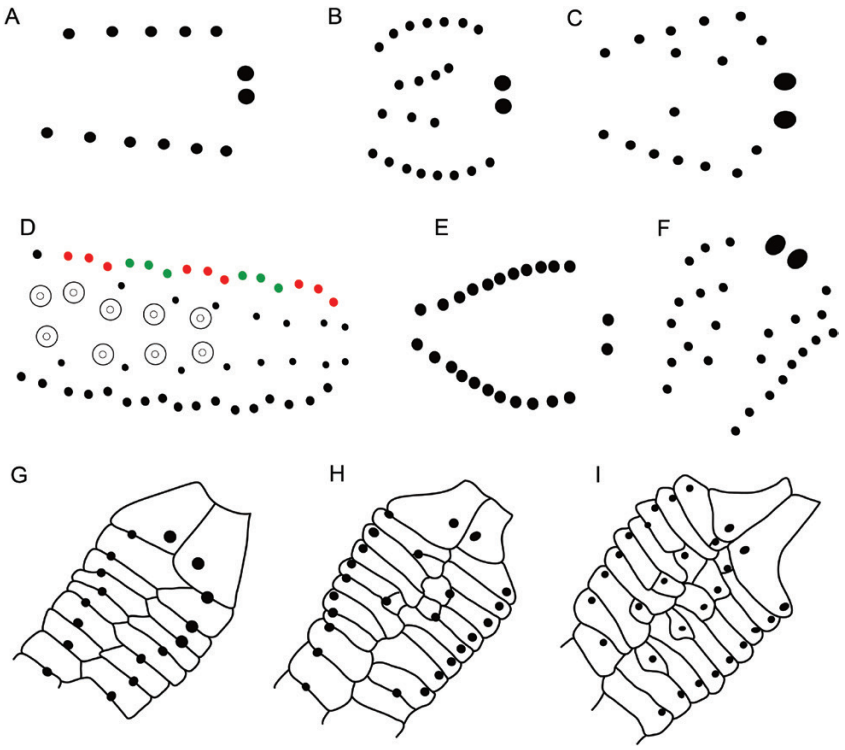

Figure 9. A–F drawings of phyllopores from the anterior paired (A–E; red and green in D indicate rows of three pores) and the posterior (F) phyllodes; buccal pores on the right; concentric circles represent primary tubercles. G–I, drawings of posterior phyllodes; basicoronal plates on the right. Drawings were based on *Oligopodia epigonus* (CASIZ 188760; A), *Hardouinia bassleri* (USNM 464461; B), *Cassidulus mitis* (ZUEC 11; C), *Apatopygus recens* (USNM E14626; D), *Hardouinia mortonis* (USNM PAL 464507; E), *Rhyncholampas pacifica* (CASIZ 90705; F), *Cassidulus mitis* (ZUEC 11; G), *Petalobrissus cubensis* (USNM PAL 131265A; H) and *Eurhodia rugosa* (USNM 264590; I). Modifications were made to some drawings to illustrate various character states. Images refer to characters 75, 76, 78–80 and 84–87.

found in the middle of the plate or near the perradial suture. These pores were considered as part of the outer column because they are not homologous with pores in occluded plates.

85. Phyllodes tapering: no [0]; yes (Fig. 9E) [1]. In tapering phyllodes, the last phyllopores are very close to each other.
86. Occluded plates in posterior phyllodes: absent or rare (Fig. 9G) [0]; few (Fig. 9H) [1]; many (Fig. 9I) [2]. The presence and number of occluded plates is usually conserved within a species, but in some cases we found one or two specimens with one occluded plate even though occluded plates were absent for the species. These occurrences were considered rare. The abundance of occluded plates was also assessed by taking the ratio between the number of occluded plates and the number of primary plates into account. In phyllodes coded as having many occluded plates, at least one-third of the plates are occluded.
87. Presence of primary tubercles on phyllodes: absent [0]; present aborally (Fig. 9D) [1].

Q) Oral ambulacra: sphaeridia.

88. Location of sphaeridial pits in posterior phyllodes: near buccal pores only [0]; throughout phyllodes [1]. This character was coded as unknown for three species (*K. malayana*, *K. florescens* and *Rp. marmini*) because they have very short phyllodes, making it challenging to assess whether the sphaeridial pits are restricted to a small region near the peristome or whether they would be widespread if the phyllodes were larger.
89. Sphaeridia placement: in open pits [0]; concealed by a thin layer of stereom [1].
90. Sphaeridial pits greatly reduced: no [0]; yes [1].
91. Number of sphaeridial pits: seven or more [0]; up to six [1].

R) Oral ambulacra: plates beyond phyllodes.

92. Shape of ambulacral plates beyond phyllodes: transverse [0]; square [1]; longitudinal [2]. This character codes for the ambulacral plates in the oral region only.

S) Overall test tuberculation.

93. Tubercle size: aboral tubercles ≥ 60% as large as oral tubercles [0]; aboral tubercles < 60% diameter of oral tubercles [1].

94. Oral tubercles with bosses displaced from centre: no [0]; yes [1]. Species with enlarged areoles have larger spines on the oral region of the test that aid in locomotion.

T) Pedicellariae.

95. Teeth on blade of ophicephalous pedicellariae: teeth form an open-U blade and run down on the edges of the neck (Fig. 10A) [0]; teeth form a semi-oval blade and run down in the middle of the neck (Fig. 10B) [1]; teeth form an oval blade and are absent in the neck (Fig. 10C) [2]. Not included in A2.

96. Size of teeth on distal region of ophicephalous pedicellariae: coarse (Fig. 10B, C) [0]; fine (Fig. 10A) [1]. Not included in A2.

97. Tridentate pedicellariae blade in relationship to base: long and narrow (Fig. 10D) [0]; short and broad (Fig. 10E) [1]. Not included in A2.

98. Teeth on base of tridentate pedicellariae (Souto & Martins, 2018: table 2): absent [0]; present [1]. Not included in A2.

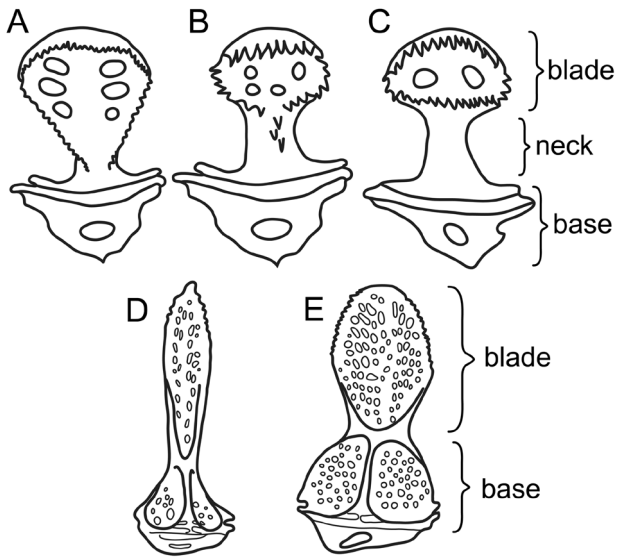

Figure 10. Drawings of ophicephalous and tridentate pedicellariae. A–C, ophicephalous pedicellariae with: A, fine teeth forming an open-U blade and running down on the edges of the neck; B, coarse teeth forming a semi-oval blade and running down in the middle of the neck; and C, coarse teeth forming an oval blade and absent in the neck. D, E, long and narrow (D) and short and broad (E) tridentate pedicellariae. Drawings were based on pedicellariae from *Neolampas rostellata* (MNHN-IE-2016-897; A), *Cassidulus mitis* (CASIZ 116110; B), *Echinolampas depressa* (CASIZ 174963; C, D) and *Cassidulus caribaearum* (CASIZ 222205; E). Modifications were made to some drawings to illustrate various character states. Images refer to characters 95–97.

A data matrix (Supporting Information, Appendix S1) was constructed in Mesquite v.3.51 (Maddison & Maddison, 2018). Phylogenetically uninformative characters were not included; polymorphic characters were retained. Inapplicable characters were coded as '–', and missing data were coded as '?'. For some characters, we were able to exclude a subset of the character states for a particular taxon, but we were unsure of the remaining character states. These partial uncertainties were included within curly brackets and not coded as missing data. We used the command 'mstaxa = variable' to differentiate partial uncertainty and polymorphism. Missing data often result in a high number of equally parsimonious solutions and reduced resolution. Partial uncertainty should ameliorate these effects.

After coding the characters, we estimated the completeness of all fossil taxa (Table 2). Rowe (1988) defined completeness as the percentage of missing data (owing to non-preservation and inapplicability) in relationship to the total number of characters in the matrix. In our estimation of completeness, only the characters with missing data owing to non-preservation were considered. We think that inapplicability should not affect the estimation of completeness, because if fossil preservation allowed for the detection of inapplicability of characters, then the preservation for that character should be considered to be good.

PHYLOGENETIC ANALYSES

Four cladistic analyses were conducted using the software PAUP* v.4.0a163 (Swofford, 2003) using the parsimony optimality criterion. In all of these, heuristic searches were performed using stepwise random addition sequences with 1000 replicates (start = stepwise, addseq = random, randomize = addseq, nreps = 100) followed by tree bisection–reconnection branch swapping (swap = tbr, multrees = yes). Five trees were held at each step of stepwise addition (hold = 5). Branches without unambiguous optimizations were collapsed (pset

collapse = minbrlen). Trees with the best score were retained (filter best = yes, permdel = yes). Finally, strict consensus and 50% majority-rule consensus trees were generated. Clade support was determined with bootstrap resampling (Felsenstein, 1985) using the full 'heuristic' option with 1000 heuristic replicates, and character changes were optimized using the 'accelerated transformation' (ACCTRAN) option. Batch files with commands are available in the Supporting Information (Appendix S2) and in Morphobank (O'Leary & Kaufman, 2012) project P3287.

Nucleolites scutatus, *Ap. recens* and *Ec. depressa* are the most distantly related taxa; hence, they were used as outgroups in PAUP to root the tree. All characters were treated as equally weighted, and continuous characters not derived from ratios were ordered (additional analyses with unordered and reweighted characters were also performed). Analysis 1 (A1) included all ingroup (45) and outgroup taxa (21), all 98 characters, and coded for partial uncertainty. To analyse the effect of missing data on the resulting topology, characters coded for < 20% of the species (N = 6) were excluded from analysis 2 (A2). In analysis 3 (A3), partial uncertainties (N = 34) were converted into missing data ('?'). Analysis 4 (A4) aimed to examine the influence of fossil taxa on the tree topology; hence, it included only extant taxa (six ingroup taxa and six outgroups).

Using stratigraphy to choose the best tree

Temporal data have been applied in parsimony-based phylogenetic reconstruction in two different ways: a priori, as discrete characters used to build phylogenies [e.g. stratocladistic methods (Bodenbender & Fisher, 2001)]; and a posteriori, as a separate dataset to test phylogenetic hypotheses (e.g. Day *et al.*, 2016). Although many agree that temporal data should be used in association with phylogeny (Gauthier *et al.*, 1988; Huelsenbeck, 1994; Fox *et al.*, 1999), stratocladistics has been severely criticized, especially because the concept of homology does not apply to time, but also because of the way that time is binned into stratigraphic intervals (Smith, 2000; Sumrall & Brochu, 2003). Fisher (2008) reviewed the main concerns raised by critics and provided a discussion addressing them. However, most software does not support temporal data, making the implementation and testing of this method challenging.

Here, we used temporal data a posteriori to calculate four stratigraphic congruence metrics [the gap excess ratio (GER; Wills, 1999; Wills *et al.*, 2008), the modified Manhattan stratigraphic measure (MSM*; Siddall, 1998; Pol & Norell, 2001), the relative consistency index (RCI; Benton & Storrs, 1994) and the stratigraphic consistency index (SCI; Huelsenbeck, 1994)] for each MPT and determine which MPT best fits stratigraphy. Different metrics of stratigraphic congruence and their refinements have been proposed, all assessing whether the FAD of a taxon corresponds to its placement in the phylogeny and/or the length of the ghost lineages.

Tests were performed using the DatePhylo and StratPhyloCongruence functions of the 'strap' R package (Bell & Lloyd, 2015). Input files consisted of the MPTs and a list with the FAD and LAD of each taxon. We adopted a conservative approach and included uncertain ages in the temporal range of species (see Table 2). Analyses were performed using the 'basic' dating method (Smith, 1994), which sets the root length at 0 Myr. Polytomies were treated as hard (hard = TRUE), and outgroups and topologies were fixed. Given that the temporal data come from stratigraphic intervals rather than absolute ages, we treated FADs and LADs as uncertain, and two values were randomly drawn from within the interval (randomly.sample.ages = TRUE, samp.perm = 1000). Estimated P-values were then calculated for these metrics from 1000 randomly generated trees (rand.perm = 1000). The R script to estimate the stratigraphic congruence metrics is provided in the Supporting Information (Appendix S2) and in Morphobank (O'Leary & Kaufman, 2012) project P3287.

Tree calibration

Stratigraphic ranges of species (Table 2) were obtained from the literature and museum records; absolute dates were not available. Five additional extinct taxa [*Paralampas platisterna* (Smith & Jeffery, 2000), *Rhyncholampas cookei* Sanchez-Roig, 1952, *Rhyncholampas fontis* (Cooke, 1942), *Rhyncholampas smithi* Srivastava *et al.*, 2008 and *Glossaster* ? *apianus* (Besaire & Lambert, 1930)] were used to calibrate the phylogeny. For each cassidulid genus, we targeted the oldest species and species occurring in different geographical areas. However, we included only the five species whose literature data allowed for a reliable phylogenetic placement. These species were manually added a posteriori to the best tree using assignable synapomorphies (e.g. node dating; Table 4), which was then calibrated using the 'basic' method and plotted against the geological time scale of the International Commission on Stratigraphy (Cohen *et al.*, 2013; updated).

RESULTS

The complete parsimony analysis including all species, characters and partial uncertainties (A1; Fig. 11) resulted in 24 MPTs of 750 steps (CI = 0.237, RI = 0.604) recovered from two tree-islands (for results with

Table 4. List of taxa chosen a posteriori to aid phylogenetic calibration, their stratigraphic range, geographical distribution, clade assigned and characters used for assignment

Taxon	Estimated age (Mya)[1]	Reference for age assignment	Geographical distribution	Clade assigned	Diagnosable character states and characteristics
Order Cassiduloida					
Paralampas platisterna	72.1–66	Smith & Jeffery (2000)	Oman and United Arab Emirates	*Paralampas*	21(1), 34(2), 44(0/1), 79(1), 81(2)
Family Cassidulidae					
Rhyncholampas cookei	37.8–33.9	Sanchez Roig (1952)	Cuba	*R. tuderi*	26(1), 29(1), 27(0), 53(1)
Rhyncholampas fontis	[66–47.8]	Cooke (1942)	USA (FL)	*R. alabamensis*	1(0), 4(0), 5(1), 10(0), 26(1), 29(1)
Rhyncholampas smithi	44–42.9	Srivastava *et al.* (2008)	India	*R. rodriguezi*_A	1(0), 4(1), 5(1), 10(0), 26(1), 29(1), petal III short
Family Faujasiidae					
Glossaster? *apianus*[2]	56–47.8	Besaire & Lambert (1930)	Madagascar	*Glossaster*	1(1&2), 39(0), 44(0), 55(2)

Genus and family classification follow the classification proposed herein. Uncertain age is given in square brackets; uncertain character states are separated by a forward slash.
[1]According to Cohen *et al.* (2013; updated).
[2]This species was originally described in the genus *Procassidulus*, but the species description and poor illustrations indicate that it has a mostly elongated test shape, an aboral and longitudinal periproct, and a deeply pitted naked zone. Also, the peristome is anteriorly placed, at ~43% of the TL from the anterior ambitus. These characteristics suggest that *Pr. apianus* should be placed within *Glossaster*, but analysis of the holotype is necessary to support this classification.

unordered and reweighted characters, see Supporting Information, Appendices S3 and S4). Low P-values for all four stratigraphic congruence metrics (Supporting Information, Appendix S5) indicate that the 24 MPTs have a better stratigraphic fit than the 1000 randomly generated trees. Three of the MPTs obtained the best fit for all four metrics; the only difference among them concerns the placement of *Eu. baumi* and its relationship to other *Eurhodia* species. The selected topology is the MPT with best stratigraphic fit and whose relationships are present in most MPTs (Fig. 12). When characters with a high percentage of missing data were removed (A2), 24 MPTs of 738 steps (CI = 0.230, RI = 0.602) were recovered. The topology of the strict (Fig. 11) and majority-rule consensuses (Fig. 13) does not change if compared with A1. Therefore, the removal or inclusion of these characters has no impact on the topology recovered in A1.

About 33% of the taxa had characters coded as partial uncertainties, varying from one to three characters in each taxon (Table 2). When partial uncertainties were converted to missing data (A3), 20 MPTs of 746 steps (CI = 0.239, RI = 0.605) were recovered. Although the major structure of the topology did not change, the relationship within some subclades changed considerably (Fig. 13B); the monophyly of genus *Eurhodia*, for example, was not supported by this analysis. These subclades comprise nine of the 22 taxa with partial uncertainties, including all taxa with three partial uncertainties. The nature of the characters may have also played a major role in recovering the topology, because the two characters with the highest number of partial uncertainties are quantitative. Analysis 3 recovered fewer MPTs than A1 and A2. Unlike partial uncertainties or any coded character, missing data do not affect tree topology. Given that most characters have a high homoplasy index, and missing data are not counted towards homoplasies, partial uncertainties return more conflicting tree solutions than missing data. Nevertheless, converting partial uncertainties into missing data removes information and should not be favoured. In the cassidulid tree recovered here, A1 has slightly better resolution than A3.

Analysis 4 (extant taxa only) was based on 70 parsimony-informative characters and resulted in four MPTs of 203 steps (CI = 0.567, RI = 0.564; Fig. 14). The relationships among the extant species changed with the removal of fossil taxa, especially regarding the

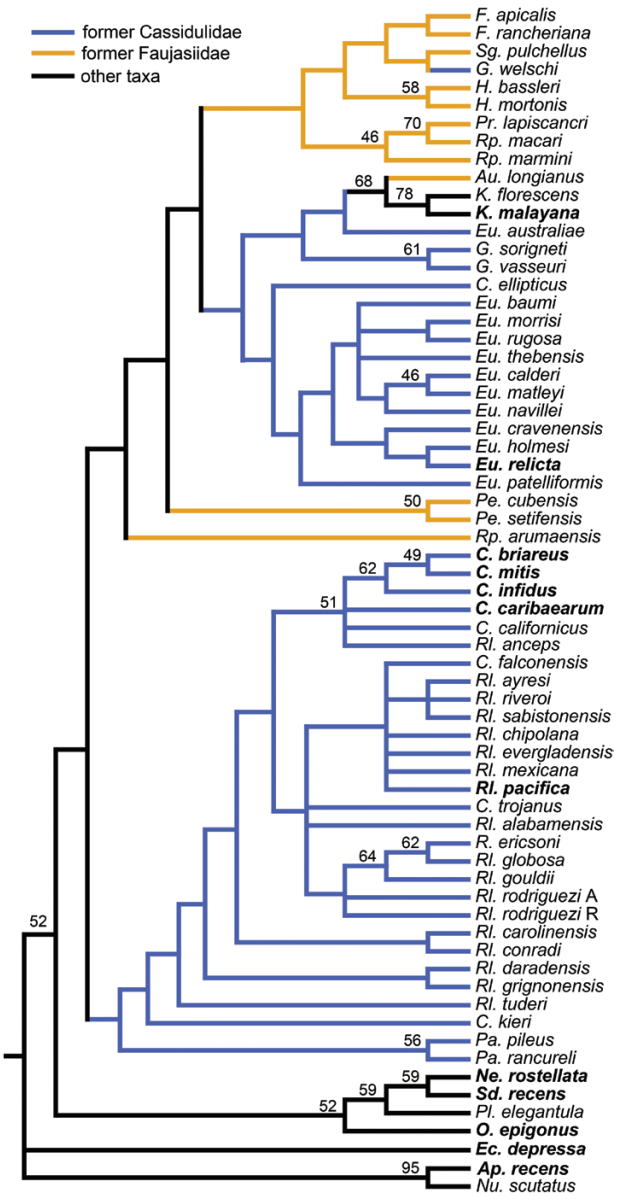

Figure 11. Strict consensus of 24 MPTs recovered by analyses 1 (including all taxa, all characters and partial uncertainty) and 2 (without characters with > 80% of missing data). Bootstrap values (1000 replicates) > 40% are shown near the nodes. Colour in lineages represents: the former cassidulids in blue, the former faujasiids in orange and other taxa in black. Extant taxa in bold.

position of *O. epigonus* and *Eu. relicta*. Also, despite the higher CI, the topology restricted to extant taxa did not add much to our knowledge of the relationship among the cassiduloid genera.

Overall, the branch support for most clades is low and does not change significantly among the four analyses.

DISCUSSION

Phylogenetic structure and taxonomic implications

Eight unambiguous synapomorphies support the clade composed by cassidulids, neolampadids and faujasiids (clade A; Table 5); five of them are related to the reduction of the phyllodes. Three major clades are then defined in the strict consensus, with the faujasiids being more closely related to the cassidulids than the neolampadids (Fig. 11). These findings contrast with the relationships recovered in previous studies (Fig. 1). In their analysis of the post-Palaeozoic echinoids, Kroh & Smith (2010) initially found a similar result, with the faujasiids sister to the cassidulids. However, after revising their analyses, the faujasiids were placed outside their cassiduloid clade [see Kroh & Smith, 2010: fig. 5 (pre-revision topology) vs. fig. 2 (post-revision topology); A. Kroh, pers. comm.]. Given the close relationship among cassidulids, faujasiids and neolampadids found here and in previous studies, our recommendation is to keep the faujasiids in the order Cassiduloida.

Clade B, composed of *O. epigonus* and the Neolampadina (neolampadids and pliolampadids), is supported by six unambiguous synapomorphies, including the placement of the ocular plates beyond the gonopores, a longitudinal peristome and further reduction of the phyllodes. Despite the placement of *O. epigonus* as sister to the Neolampadina, an analysis with additional neolampadids and gitolampadids is necessary to better classify this species as a member of this subfamily or of another clade. For now, we rule out the possibility of *O. epigonus* being a member of the Cassidulidae (as suggested by Mortensen, 1948a; Mooi, 1990b), but this species is likely to be a cassiduloid (from here onwards *sensu* this paper, unless stated otherwise) closely related to the Neolampadina. The suborder Neolampadina (clade C) is supported by eight unambiguous synapomorphies, including the funnelled posterior region, the loss of gonopore 3 and the presence of six plates on I5 up to the plates framing the periproct.

Clade D is supported by five unambiguous synapomorphies, including the shape of the ophicephalous pedicellariae (with teeth forming a semi-oval blade and running down the middle of the neck) and the presence of a developed naked zone in I5 and ambulacrum III. The monophyly of the family Cassidulidae *sensu* Kroh & Mooi (2018) (see Table 1) is not supported, because the genera *Eurhodia* and *Glossaster* are placed in an external clade.

Clade E is composed of two subclades, one of them composed of faujasiids (clade F) and another composed of genera previously belonging to the cassidulids and a faujasiid (clade G). Clade E is

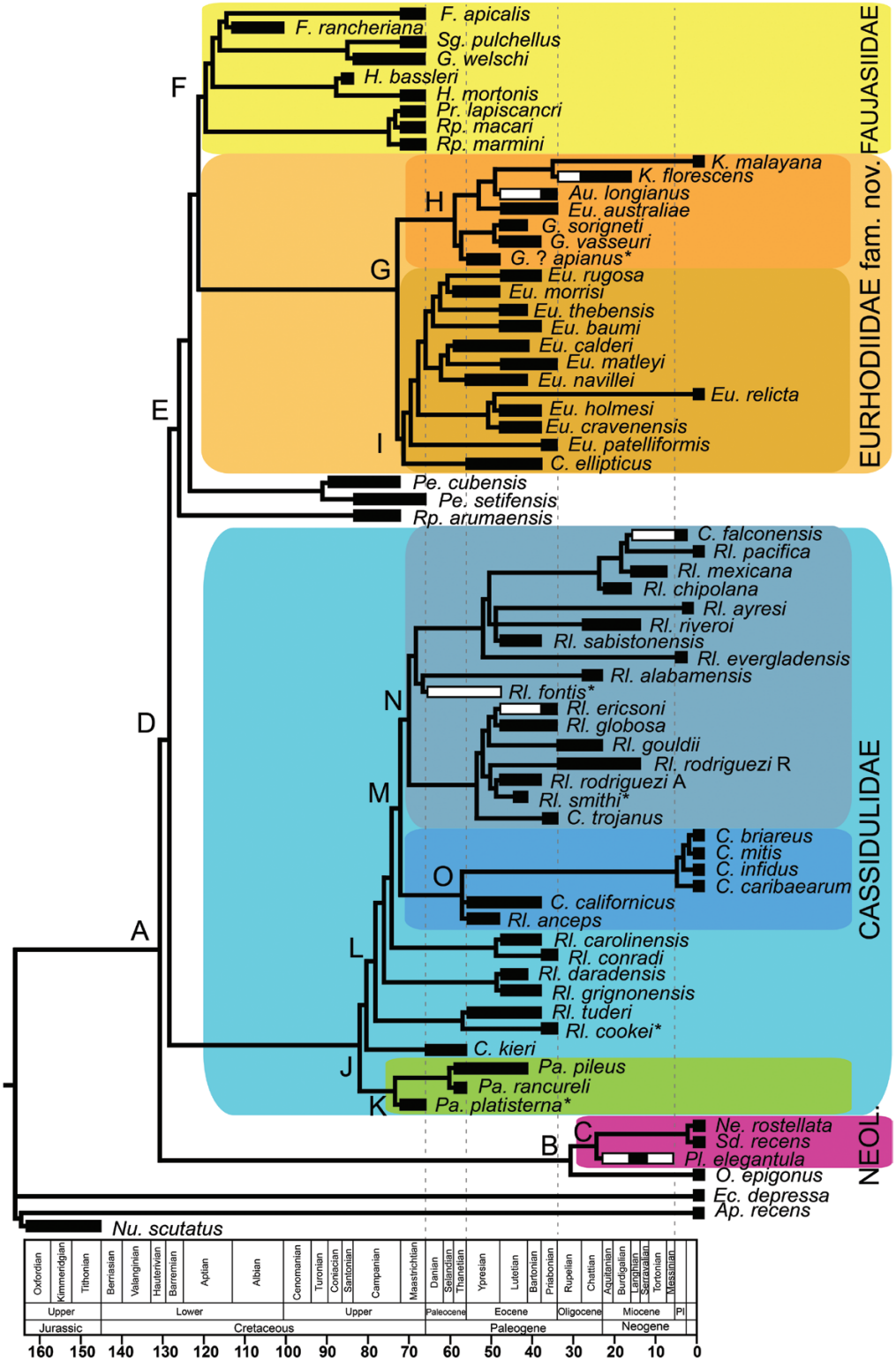

Figure 12. Preferred tree topology with best stratigraphic congruence from analysis 1 and proposed designation for the families Cassidulidae (in blue), Eurhodiidae (in orange) and Faujasiidae (in yellow). Other taxa highlighted here are the genus *Paralampas* (in green) and the suborder Neolampadina (NEOL.; in pink). Calibration was performed with the 'basic' method (Smith, 1994) and includes the stratigraphic range of species added a posteriori (*). Clades discussed in the text are indicated by capital letters. Black bars represent known stratigraphic ranges and white bars represent uncertain range.

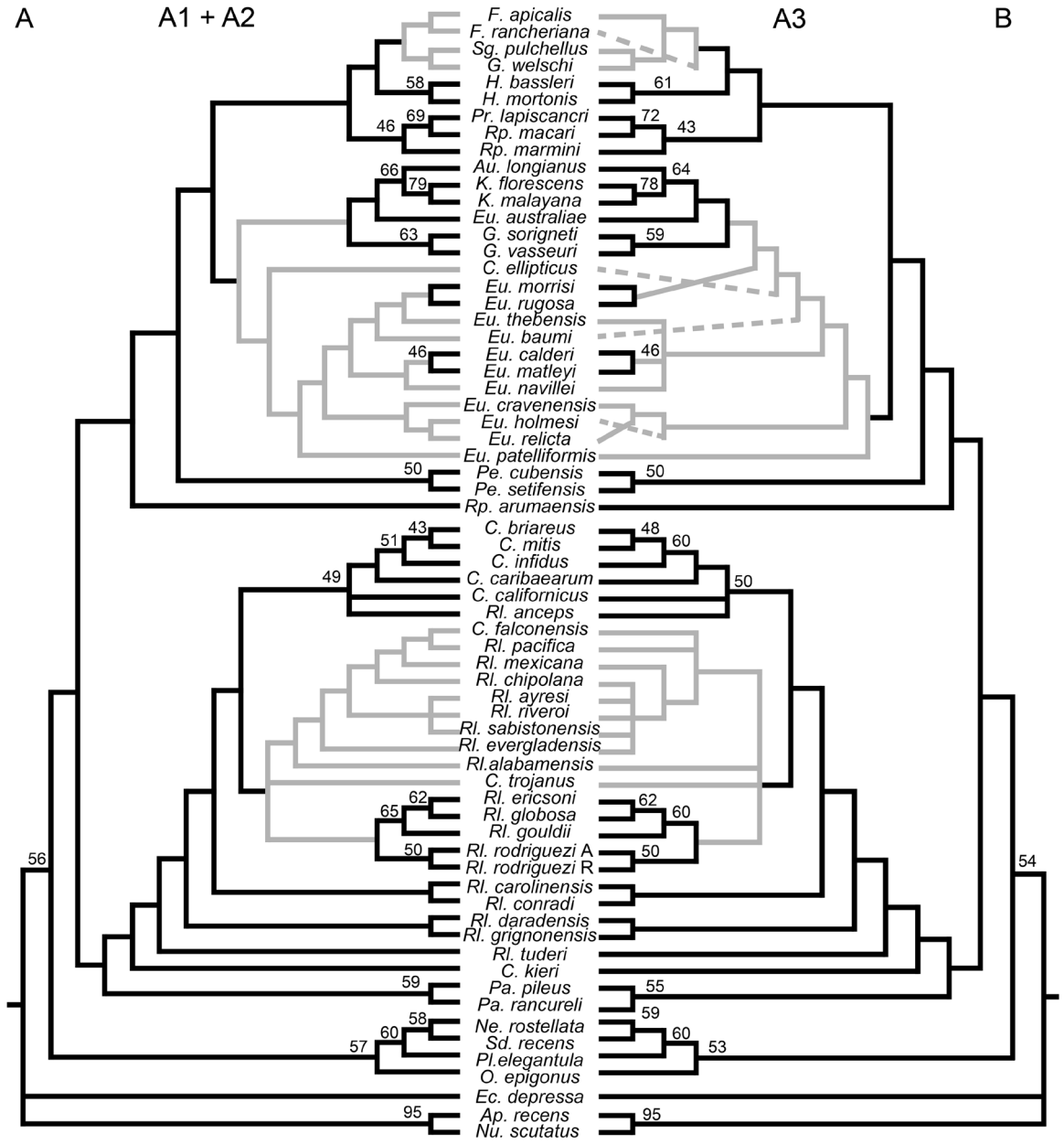

Figure 13. Fifty per cent majority-rule consensus of: A, 24 MPTs recovered by analysis 1 (including all taxa, all characters and partial uncertainty) and analysis 2 (without characters with > 80% of missing data); and B, 20 MPTs recovered by analysis 3 (partial uncertainties as missing data). Bootstrap values (1000 replicates) > 40% for analysis 2 and analysis 3 are shown near the nodes. Differences between cladograms are in light grey.

supported by seven unambiguous synapomorphies related to the size and shape of the basicoronal plate 5 and to the number of occluded plates in the posterior phyllodes. Regarding the evolution of the phyllodes, morphological data indicate that the Neognathostomata phyllode was initially composed of a single column of plates per half and with pores in triads (Fig. 9D). Long phyllodes with single columns are found in apatopygids and most echinolampadids, although their phyllopores are not organized in a uniform column when observed from the outside of the test. At some point, occluded plates evolved, possibly with the reduction of plates in the triads. For instance, the plates in *Ap. recens* vary in size and shape, and some phyllopores are placed near the perradial suture. Taxa from clade E usually have many occluded plates in the phyllodes, whereas cassidulids and neolampadids tend to have fewer.

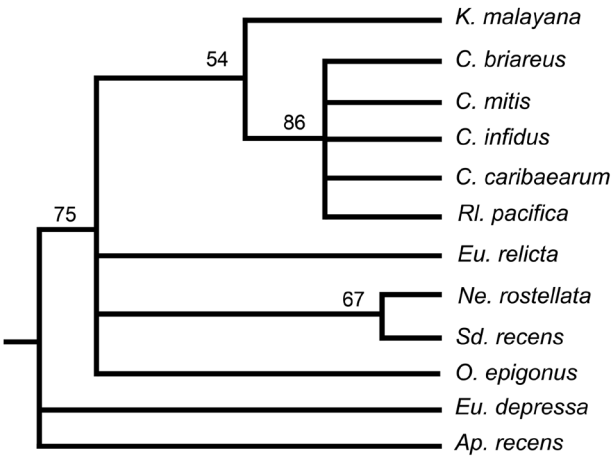

Figure 14. Fifty per cent majority-rule consensus of four MPTs recovered by analysis 4 (extant taxa only). Bootstrap values (1000 replicates) > 40% are shown near the nodes.

Based on our morphological analyses, the taxa belonging to clade G are unique and different enough from the faujasiids (clade F) to justify the level of family. In addition to its morphological distinctiveness, the decision to constrain the faujasiids to clade F and describe a new family for clade G is an attempt to stabilize the taxonomy of the family Faujasiidae. Smith & Wright (2000) subdivided the faujasiids into two subfamilies mainly based on the position of the periproct: marginal to inframarginal in the Faujasiinae and supramarginal to aboral in the Stigmatopyginae. Our analyses do not support the subfamily Stigmatopyginae, because this subfamily is based on plesiomorphic characters and its members do not form a monophyletic group. Also, its type genus, *Stigmatopygus*, is resolved as immediate sister to *Faujasia*. As a result, retention of Stigmatopyginae would require the description of at least two additional subfamilies in the Faujasiidae (i.e. one for the clade with *Hardouinia* and another for the clade with *Procassidulus* and *Rhynchopygus*), all with only a few genera.

Clade F, composed of faujasiids, is supported by five unambiguous synapomorphies related to the adoral region, including the shape of the basicoronal plate 5 (i.e. adorally depressed and aborally elongated), presence of tooth-like bourrelets and reduction of the buccal pores. The former two synapomorphies are also present in *Au. longianus*, placed within clade H. Tooth-like bourrelets have been used to diagnose the family Faujasiidae, but some faujasiids (e.g. *F. rancheriana*) do not possess this trait. According to the present phylogeny, tooth-like bourrelets evolved at least twice, and there was at least one reversal to a previous state.

Five unambiguous synapomorphies support Eurhodiidae fam. nov. (clade G), including having a monobasal apical system, pits on the interambulacral basicoronal plates, and pointed bourrelets. Two subclades split in clade G, each supported by two unambiguous synapomorphies: clade H contains *Au. longianus*, *Eu. australiae*, *Glossaster* and *Kassandrina*; and clade I is composed of *C. ellipticus* and the other *Eurhodia* species. Some characteristics that ditinguish them are, respectively, a longitudinal vs. a transverse periproct, anterior paired petals oval vs. leaf-shaped and eight or more vs. eight or fewer plates framing the periproct. The topology of clade G changed considerably when partial uncertainties were converted into missing data. Although relationships within clade H did not change, clade I collapsed, and support for the monophyly of the genus *Eurhodia* was lost.

The genus *Eurhodia* displays some of the greatest diversity in test shape within the cassiduloids, and three genera have been described to separate its valid species: *Eurhodia*, for the species *Pygorhynchus morrisi*; *Ravenelia* McCrady, 1859, for the species *Pygorhynchus rugosus*; and *Gisopygus* Gauthier in Fourtau, 1899, for four Egyptian species described as *Rhynchopygus*, amongst them, *Rp. navillei* and *Rp. thebensis* (note also that Kier, 1962, doubtfully considered this genus a synonym of *Rhyncholampas*, although he did not analyse any specimens). The results recovered here do not support any of these genera. Also, no other *Eurhodia* species strongly resembles its type species, *Eu. morrisi*, and few of the currently valid *Eurhodia* species were originally described in this genus. Despite the uniqueness of *Eu. morrisi* and the lack of non-homoplastic synapomorphies supporting clade I, we decided to maintain all species in this clade within the genus *Eurhodia* to maintain its stability.

In addition to revealing a new cassiduloid family, other taxonomic implications stem from the relationships recovered in clade E. Firstly, the genus *Rhynchopygus* is characterized by a prominent extension above the periproct that is absent in both *Rp. arumaensis* and *Rp. macari*. *Rhynchopygus arumaensis* split off early in the evolution of clade E and should be placed in a different genus. *Rhynchopygus macari* shares more characters with *Pr. lapiscancri* than with *Rp. marmini*, suggesting that they could all belong to the same genus or to different genera. But an analysis of the other *Rhynchopygus* and *Procassidulus* species is needed to verify the variability within each of these genera before any conclusion is drawn. Secondly, although *F. apicalis* and *F. rancheriana* are sister taxa, our morphological analyses reveal that *F. rancheriana* has characteristics diagnostic of the genus *Eurypetalum* Kier, 1962 (i.e. rounded bourrelets and a tetrabasal apical system vs. tooth-like bourrelets and monobasal apical system in *Faujasia*), and thus *F. rancheriana* is transferred to this genus, i.e. *Eurypetalum rancheriana* comb. nov.

Table 5. Apomorphy list for the clades labelled in Figure 12

Clade	Character	Change	Clade	Character	Change	Clade	Character	Change
A	9	0 → 1	D	27	0 ⇒ 1	I	21	0 ⇒ 1
	13	0 → 1		51	1 → 0		36	2 → 0
	34	0 → 1		52	0 ⇒ 2		43	0 ⇒ 1
	37	0 ⇒ 1		57	0 ⇒ 2	J	41	0 ⇒ 1
	39	0 → 1		79	0 ⇒ 2		46	0 → 1
	74	1 ⇒ 0		95	0 ⇒ 1		47	0 → 1
	77	0 ⇒ 1	E	9	1 → 0		55	0 → 1
	81	0 ⇒ 1		12	1 ⇒ 0		67	0 ⇒ 1
	82	0 ⇒ 1		19	1 ⇒ 0	K	21	0 ⇒ 1
	83	0 ⇒ 1		32	0 ⇒ 1		34	1 ⇒ 2
	91	0 ⇒ 1		36	2 → 0		44	0 ⇒ 1
	92	0 ⇒ 2		68	0 ⇒ 1		79	2 ⇒ 1
	97	0 → 1		69	0 ⇒ 1		81	1 ⇒ 2
B	4	0 → 1		78	0 ⇒ 2		83	1 ⇒ 2
	6	0 → 1		86	0 ⇒ 2	L	26	0 → 1
	8	1 → 0	F	19	0 → 2		29	0 ⇒ 1
	16	0 ⇒ 1		34	1 → 2		37	1 ⇒ 0
	22	2 ⇒ 1		65	0 ⇒ 1		44	0 ⇒ 2
	49	3 → 4		70	0 → 1		48	0 ⇒ 1
	58	0 ⇒ 2		71	0 ⇒ 1		61	0 → 1
	70	0 ⇒ 1		73	0 ⇒ 1		93	0 ⇒ 1
	81	1 ⇒ 2		75	2 ⇒ 1	M	9	1 ⇒ 0
	83	1 ⇒ 2		76	0 ⇒ 1		53	0 ⇒ 1
	94	1 → 0	G	1	1 ⇒ 2		72	0 ⇒ 1
	96	0 → 1		12	0 ⇒ 1		89	0 → 1
C	3	0 ⇒ 1		22	2 → 1	N	21	0 → 1
	14	0 ⇒ 1		55	0 ⇒ 2		36	2 ⇒ 1
	23	1 ⇒ 0		56	0 ⇒ 1		49	3 ⇒ 2
	25	3 ⇒ 0		64	0 ⇒ 1		63	0 ⇒ 1
	32	0 → 1	H	23	1 → 0		91	1 ⇒ 0
	48	0 → 1		25	4 → 2	O	27	1 ⇒ 0
	49	4 ⇒ 5		39	1 → 0		32	2 → 1
	66	0 ⇒ 1		44	2 → 0		55	1 ⇒ 2
	68	0 ⇒ 1		50	3 ⇒ 1		79	1 ⇒ 0
	79	0 → 1		88	0 ⇒ 1		83	1 ⇒ 2
	81	2 → 3		97	1 → 0		86	1 → 0
	86	0 ⇒ 1						

Single arrows (→) indicate ambiguous synapomorphies, and double arrows (⇒) indicate unambiguous synapomorphies. Major clades are as follows: A, Cassiduloida; C, Neolampadina; F, Faujasiidae; G, **Eurhodiidae fam. nov.**; I, *Eurhodia*; J, Cassidulidae; K, *Paralampas*; M, crown group Cassidulidae; N, *Rhyncholampas*; O, *Cassidulus*.

Thirdly, *Eu. australiae* is unlike any other *Eurhodia* species we analysed (e.g. oval petals; longitudinal, narrow and almost aboral periproct) and should be placed in a genus different from the ones included in this phylogeny. Alternatively, *C. ellipticus* should be transferred to *Eurhodia*. Finally, *G. welschi* should be assigned to another genus because the type species of *Glossaster*, *G. sorigneti*, and other analysed *Glossaster* species are placed in a different clade. Smith & Jeffery (2000) transferred *G. welschi* to the genus *Stigmatopygus*, and our analyses support this change.

The family Cassidulidae (clade J), composed of the genera *Paralampas* (clade K), *Rhyncholampas* (clade N) and *Cassidulus* (clade O), is supported by two unambiguous synapomorphies: plates framing the periproct do not bend inwards, and basicoronal

plates 1 and 4 are narrower than basicoronal plate 5. Five early dichotomies split the stem from the crown group Cassidulidae. Stem group Cassidulidae is composed of *Paralampas*, *C. kieri* and three other lineages, each with two species of *Rhyncholampas*. These species, or species pairs, should be reassigned to new genera. However, because each species in a lineage (e.g. *Rl. carolinensis* and *Rl. conradi*, *Rl. daradensis* and *Rl. grignonensis*) has many apomorphies, additional morphological analyses are needed to determine whether each lineage is made up of one genus or if each species should be placed in a new genus. Also, we analysed ~38–67% (Table 3) of the described *Rhyncholampas* species, and the species not included in the present study might shed light on this taxonomic revision. The genus *Paralampas* (clade K) is supported by six unambiguous synapomorphies, including posterior ambulacra with strong expansion beyond petals, periproct equant, anterior phyllodes with five to seven primary plates, and posterior phyllodes with four to seven primary plates. The major difference between *Pa. pileus* and *Pa. rancureli* is the development of the bourrelets (poorly developed vs. strongly pointed), respectively.

The crown Cassidulidae (clade M) is supported by four synapomorphies (three unambiguous): posterior region of test not truncated, naked zone wide, basicoronal ambulacral plates bent and enclosed sphaeridial pits. Two characters coded only for extant species also support this clade, although they could have evolved at any node between clades D and M: periproctal membrane with two rows of medium-sized plates and anus placed on the aboral edge. The genus *Cassidulus* (clade O) is supported by four unambiguous synapomorphies, mostly related to the reduction of the phyllodes that have few plates, none of them occluded. The genus *Rhyncholampas* (clade N) is supported by four unambiguous synapomorphies, including having petals the same width as the ambulacra beyond petals and seven or more sphaeridia. *Rhyncholampas* is subdivided into two clades, and the placement of *C. trojanus* and *Rl. alabamensis* was not the same in all MPTs (Fig. 13). Also, the conversion of partial uncertainties into missing data destabilized the relationships in this clade.

Morphological differences between the genera *Cassidulus* and *Rhyncholampas* are slight, although they diverged > 60 Mya. Many *Rhyncholampas* species were originally placed in the genus *Cassidulus* and later transferred to *Rhyncholampas*. This analysis corroborates some of these taxonomic assignments (i.e. *Rl. alabamensis*, *Rl. ericsoni*, *Rl. evergladensis*, *Rl. globosa*, *Rl. mexicana*, *Rl. riveroi*, *Rl. sabistonensis*) and includes *C. falconensis* and *C. trojanus*, which had been previously described as and placed in *Eurhodia*, respectively. These results also indicate that *Rl. anceps* should be placed in the genus *Cassidulus*, and the *Rhyncholampas* species outside of clade M and *C. kieri* should be placed in other genera.

REVISED TAXONOMY OF THE CASSIDULOIDS ANALYSED IN THE PRESENT STUDY

Below is a revised classification of the cassiduloids based on our phylogenetic hypothesis and diagnoses for the supraspecific taxa included in the ingroup. Given that we included only a few species of Faujasiidae and Neolampadidae, we did not provide diagnoses for these. Owing to the mosaic evolution displayed by many of these taxa, as evidenced by the phylogenetic analysis, the diagnoses presented here are based on unique combinations of characters, which should not be considered in isolation.

Order Cassiduloida Agassiz & Desor, 1847

Emended diagnosis: Neognathostomata with an anterior apical system with three (G3 missing) or four gonopores. Peristome anterior; buccal pores developed. Bourrelets formed only by the basicoronal plate and never flush. Phyllodes developed; short (i.e. adradial to third plate of interambulacra 1 and 5). Ambulacral basicoronal plates with up to two pores; second pore placed aborally and near adradial suture. Sphaeridia few (usually up to six, no more than eight). Perignathic girdle lacking; lantern present only in very early life stages.

Included families based on present analysis: Cassidulidae, Eurhodiidae fam. nov., Faujasiidae, Neolampadidae and Pliolampadidae.

Family Cassidulidae Agassiz & Desor, 1847

Emended diagnosis: Cassiduloids with monobasal apical system. Pore-pairs conjugated by slight or sharp furrow. Ambulacral plates following posterior petals usually wider than long, with pores placed towards adradial suture. Periproct supramarginal, equant or transverse. Plates framing periproct not bending inwards; interambulacral plates adoral to periproct convex. Naked zone present in ambulacrum III and interambulacrum 5; pits small or absent. Phyllodes medium-sized to long; occluded plates absent or scattered. Peristome equant or transverse; (sub)pentagonal. Interambulacral basicoronal plates 1 and 4 narrower than interambulacral basicoronal plate 5. Bourrelets

poorly developed, bulged or pointed; formed by accretion of stereom onto basicoronal plates. Sphaeridia placed near buccal pores. Oral tubercles much larger than aboral tubercles. From living species of *Cassidulus* and *Rhyncholampas*: periproctal membrane with two rows of medium-sized plates and few small plates; anal opening on aboral edge. Tridentate pedicellariae short, broad.

Type genus: Cassidulus Lamarck, 1801

Included genera based on present analysis: Cassidulus, *Paralampas* and *Rhyncholampas*.

Misclassified cassidulids in need of reassignment after additional studies: C.? kieri, *Rl.? carolinensis*, *Rl.? conradi*, *Rl.? cookei*, *Rl.? daradensis*, *Rl.? grignonensis* and *Rl.? tuderi*.

Genus *Cassidulus* Lamarck, 1801

Emended diagnosis: Small to medium-sized cassidulids with oval test; oral region concave. Anterior petals tulip-shaped (or rarely straight); posterior petals straight. Paired petals with unequal number of pores in a and b columns (difference up to four pore-pairs in anterior paired petals, up to six pore-pairs in posterior paired petals). Poriferous zones with sparse primary tubercles. Periproct transverse, with prominent aboral hood. Six to eight interambulacral plates between basicoronal plate 5 and base of periproct. Interambulacrum 5 naked zone wide; pits abundant, large or small. Anterior phyllodes with five to ten phyllopores per half; posterior phyllodes with four to seven phyllopores per half; occluded plates lacking. Bourrelets poorly developed or bulged. Sphaeridia concealed by thin layer of stereom (fossils could have lost pit covering or pits in some species possibly open).

Included species based on present analysis: C. caribaearum (type species), *C. anceps* comb. nov., *C. briareus*, *C. californicus*, *C. infidus* and *C. mitis*.

Genus *Paralampas* Duncan & Sladen, 1882

Emended diagnosis: Small cassidulids with oval and inflated test; oral region of test slightly concave. Petals long (petal III longest), broad; outer column bowed, a and b columns of pore-pairs with equal number of pores; poriferous zone wide, lacking primary tubercles. Anterior paired petals tulip-shaped. Plates immediately after posterior petals squared and then widened, greatly increasing ambulacral width. Periproct equant, framed by seven or eight plates. About seven or eight interambulacral plates between basicoronal plate 5 and adoral base of periproct. Interambulacrum 5 naked zone narrow; pits small or absent. Outer column of phyllodes with four to seven phyllopores per half; occluded plates few or absent. Bourrelets poorly developed or pointed.

Included species based on present analysis: Pa. pileus (type species), *Pa. platisternus* and *Pa. rancureli*.

Genus *Rhyncholampas* Agassiz, 1869

Emended diagnosis: Small to large cassidulids of varying test shape. Anterior paired petals tulip- or leaf-shaped; posterior petals bowed. Paired petals with unequal number of pores in a and b columns (difference up to four pore-pairs in anterior paired petals, up to ten pore-pairs in posterior paired petals). Poriferous zones with three or more reduced primary tubercles. Periproct transverse, with prominent aboral hood. Posterior region of test sometimes truncated. Six to ten interambulacral plates between basicoronal plate 5 and base of periproct. Interambulacrum 5 naked zone usually wide, finely pitted, although pits vary from absent to large. Bourrelets bulged or pointed; bourrelet 5 often convex, projecting towards peristome. Outer column of anterior phyllodes with five to 12 phyllopores per half; posterior phyllodes with eight 12 phyllopores per half; occluded plates often scattered. Phyllopores in large specimens often disorganized throughout phyllodes. Sphaeridia concealed by thin layer of stereom (fossils could have lost pit covering or pits in some species possibly open).

Included species based on present analysis: Rl. pacifica (type species), *Rl. alabamensis*, *Rl. ayresi*, *Rl. chipolana*, *Rl. ericsoni*, *Rl. evergladensis*, *Rl. falconensis* comb. nov., *Rl. fontis*, *Rl. globosa*, *Rl. gouldii*, *Rl. mexicana*, *Rl. riveroi*, *Rl. rodriguezi*, *Rl. sabistonensis*, *Rl. smithi* and *Rl. trojana* comb. nov.

Family **Eurhodiidae fam. nov.**

Diagnosis: Cassiduloids with monobasal apical system. Outer column of anterior petals bowed, posterior petals straight or bowed, a and b columns of pore-pairs with equal number of pores; poriferous zone wide; pore-pairs conjugated. Periproct supramarginal or on aboral surface, longitudinal or transverse. Plates framing periproct bent inwards, with adoral plates sometimes forming a subanal shelf. Interambulacrum 5 naked zone wide; pits absent to large. Basicoronal plates usually pitted. Phyllodes small to long; phyllopores uniformly arranged;

occluded plates absent, scattered or forming inner column. Peristome pentagonal, (rarely) oval. Bourrelets pointed or (rarely) tooth-like, often formed by depression in basicoronal plates. Sphaeridia in open pits near buccal pores or throughout phyllodes. Oral tubercles usually much larger than aboral tubercles. From living species of *Eurhodia* and *Kassandrina*: periproctal membrane with one main row of medium-sized plates and many small plates, anal opening on aboral edge.

Type genus: Eurhodia d'Archiac & Haime, 1853.
lsid
urn:lsid:zoobank.org:pub:F724DA40-7ADE-47F8-8691-3123E89051A4

Included genera: Australanthus, *Eurhodia*, *Glossaster* and *Kassandrina*.

Misclassified eurhodiids in need of reassignment after additional studies: Eu.? australiae.

Genus *Eurhodia* d'Archiac & Haime, 1853

Emended diagnosis: Small to medium-sized eurhodiids with rounded to elongate test, usually with concave oral region, although a few species have only depressed midline. Anterior paired petals tulip- or leaf-shaped; posterior petals bowed and often largest. Poriferous zone with reduced or normal primary tubercles. Outer columns of pore-pairs in posterior petals sometimes wider than inner columns. Periproct supramarginal, transverse, with subanal shelf. Posterior region of test sometimes truncated. Five to nine interambulacral plates between basicoronal plate 5 and base of periproct. Naked zone usually deeply pitted. Peristome longitudinal, pentagonal (except for *Eu. relicta*, which has oval peristome). Bourrelets pointed, bourrelet 5 reduced. Anterior paired phyllodes with five to 13 phyllopores per half; occluded plates always present, sometimes forming inner column. Sphaeridial pits may be placed near buccal pores or throughout phyllodes, along inner column of pores.

Included species based on present analysis: Eu. morrisi (type species), *Eu. baumi*, *Eu. calderi*, *Eu. cravenensis*, *Eu. elliptica* comb. nov., *Eu. holmesi*, *Eu. matleyi*, *Eu. navillei*, *Eu. patelliformis*, *Eu. relicta*, *Eu. rugosa* and *Eu. thebensis*.

Genus *Australanthus* Bittner, 1892

Emended diagnosis: Medium-sized to large eurhodiids with rounded to oval and domed test; oral region concave. Anterior petals oval; posterior petals of uniform width. Poriferous zone very wide when compared with interporiferous zone, with three to five reduced primary tubercles. Pore-pairs from middle to end of posterior petals placed towards middle of plate. Occluded plate often present at end of paired petals. Ambulacra beyond posterior petals greatly expanded; pores placed in middle of plate, along suture. Periproct on aboral surface, narrow, longitudinal. About seven to ninve interambulacral plates between basicoronal plate 5 and base of periproct. Naked zone not pitted. Peristome equant, pentagonal. Bourrelets tooth-like. Phyllodes short; up to five phyllopores per half, lacking occluded plates. Sphaeridial pits very small, arranged in groups of three along phyllodes.

Included species based on present analysis: Au. longianus (type species).

Genus *Glossaster* Lambert, 1918

Emended diagnosis: Medium-sized eurhodiids with straight-edged, elongate test; oral region concave. Petals bowed; inner column of petal III straight. Poriferous zone wide, with sparse primary tubercles. Periproct on aboral surface, tear-shaped, longitudinal. About seven or eight interambulacral plates between basicoronal plate 5 and base of periproct. Naked zone fully pitted. Peristome longitudinal, pentagonal, placed near anterior edge of test. Bourrelets pointed; bourrelet 5 reduced. Phyllodes with about eight to 12 phyllopores per half; occluded plates present, may be scattered or forming inner column.

Included species based on present analysis: G. sorigneti (type species), *G. apianus* comb. nov. and *G. vasseuri*.

Genus *Kassandrina* Souto & Martins, 2018

Emended diagnosis: Medium-sized eurhodiids with straight-edged, oval test; oral region concave. Petals short; anterior petals oval; posterior petals of uniform width. Poriferous zone very wide when compared with interporiferous zone, with sparse primary tubercles. Ambulacra beyond posterior petals expanded; pores placed in middle of plate, along suture. Periproct on aboral surface, narrow, longitudinal. About seven to nine interambulacral plates between basicoronal plate 5 and base of periproct. Naked zone with large or small pits. Peristome transverse, pentagonal. Bourrelets pointed. Phyllodes short; up to five phyllopores per half; occluded plates scattered. Tridentate pedicellariae long, thin.

Included species based on present analysis: K. malayana (type species) and *K. florescens*.

HOMOPLASY AND CHARACTER EVOLUTION

The low CI and moderate RI (Fig. 15; Supporting Information, Appendix S6) indicate that most characters are homoplastic, which helps to explain the low bootstrap values. A similar result was obtained by Smith (2001) and Kroh & Smith (2010) in their phylogeny of the post-Palaeozoic echinoids, which suggested that the evolutionary history of the cassiduloids involved multiple shuffling of character states (shuffling here does not refer to lateral gene transfer, but to the constant character state changes as a result of homoplasy) rather than the evolution of novel traits (Smith, 2001; present paper). Kier (1962), Suter (1994a) and Saucède & Néraudeau (2006) also attributed the high level of homoplasy, and consequently low phylogenetic resolution, to parallel evolution in the cassiduloids. In fact, parallelism and reversals are frequent among irregular echinoids that evolved to live in similar environments (e.g. Kier, 1974; Smith, 2001; Saucède *et al.*, 2003).

The evolution of the apical system from four to one genital plate (i.e. tetrabasal vs. monobasal) has been poorly studied. It is unclear whether some genital plates reduced in size until they disappeared, leaving a single enlarged plate, whether the genital plates fused to form a solid plate, or whether there was some combination of these processes. In the cassiduloid clade described here, the apical system changed from monobasal to tetrabasal in some faujasiids, and then apparently reverted to monobasal in *F. apicalis*.

Other major transitions concern the peristome and periproct. In the reconstructed cassiduloid phylogeny, the orientation of the peristome changed from transverse to longitudinal and vice versa, the periproct position changed multiple times from marginal to aboral and once to oral (all within clade E), and the orientation of the periproct changed multiple times from longitudinal to transverse. These transitions are affected by the rate and orientation of plate growth and the rate of plate addition. Different lineages could be affected differently. For example, a transverse periproct is not necessarily framed by fewer plates than a longitudinal periproct, and the number of interambulacral plates from the peristome to the periproct is not necessarily higher if the periproct is aboral rather than marginal, although the number of plates tends to be lower in species whose periproct is oral (Figs. 16, 17).

Souto & Martins (2018) showed that the bourrelets in cassiduloids may be formed by the accretion of stereom onto the basicoronal plates or by an internal depression on the basicoronal plates that projects the bourrelets outwards. Our morphological analyses indicate that these conditions can also co-occur. For example, *Rl. pacifica* has a slight depression in the interambulacral basicoronal plates and a thick accretion of stereom, whereas *K. florescens* has a deep depression in the interambulacral basicoronal plates and a slight accretion of stereom. Given that slight depressions are difficult to detect in fossils and unbroken extant species, we did not code for

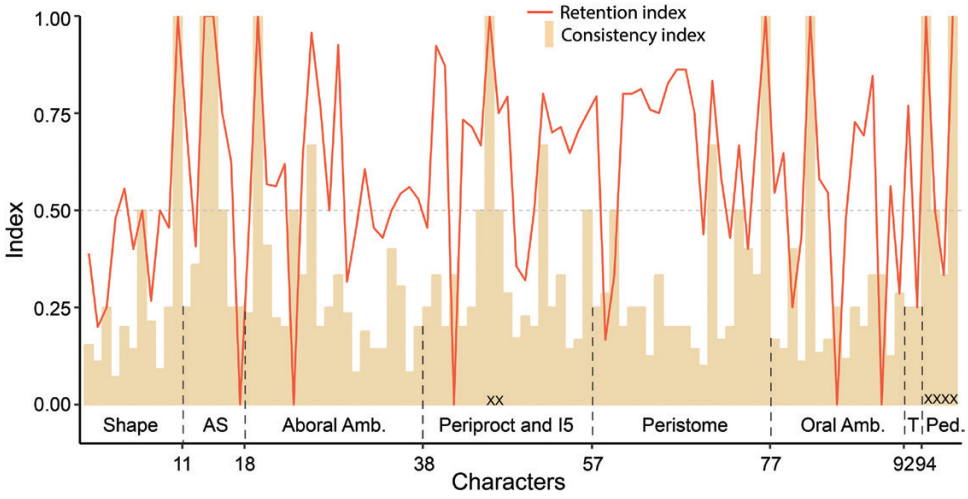

Figure 15. Plot with the consistency (bar plot) and retention (line plot) indexes for characters in analysis 1. Dashed line separates the following categories of morphological characters: test shape, apical system (AS), aboral ambulacra, periproct and interambulacrum 5, peristome and basicoronal plates, oral ambulacra, test tuberculation (T) and pedicellariae (Ped.). Characters removed from analysis 2 because of the amount of missing data are marked with an 'X'.

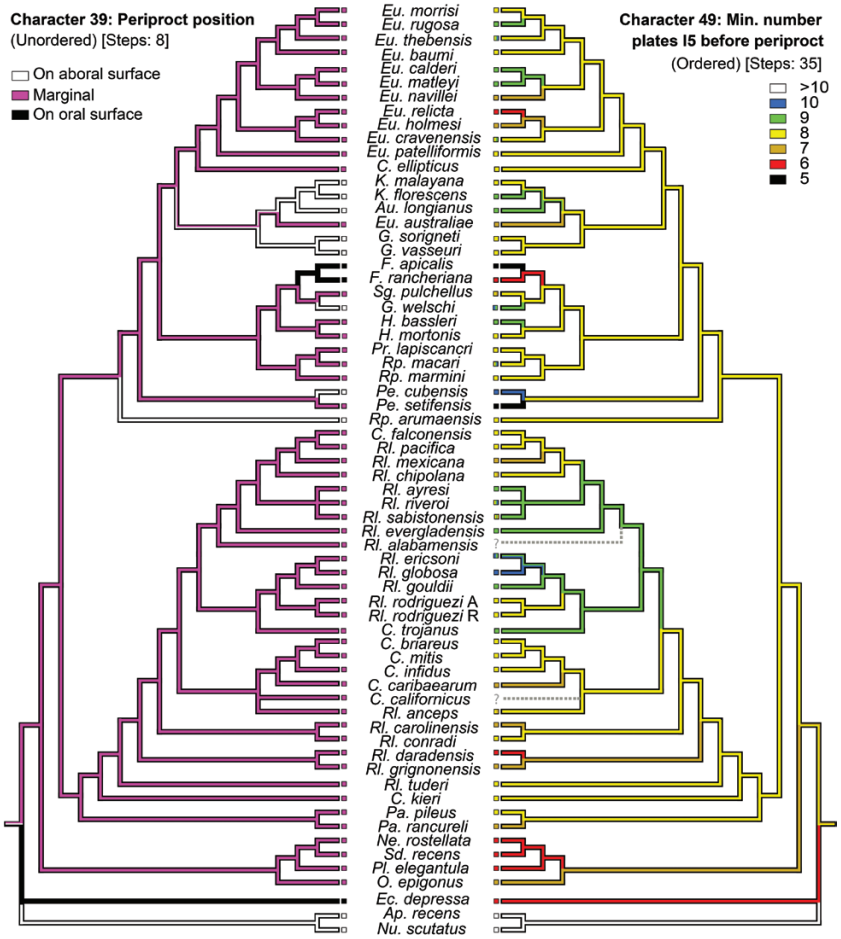

Figure 16. Mirrored trees depicting the maximum parsimony optimization of 'periproct position' on the left and 'minimum number of plates on I5, between the basicoronal plate and the base of the periproct' on the right. Branch colour refers to inferred ancestral state. Dashed grey line indicates missing data.

it. Whether both conditions co-occur or not, usually only one is responsible for the formation of the bourrelets. Usually, tooth-like and pointed bourrelets in faujasiids are formed by a deep depression in the plates, whereas the bulged and pointed bourrelets in cassidulids are formed by a strong accretion of stereom.

Micro-computed tomography has provided insights about the different ways in which bourrelets are built (Souto & Martins, 2018), but there is still much to learn about other cassiduloid novelties, such as modifications of the naked zone and apical system. These novelties are usually coded for presence vs. absence or tetrabasal vs. monobasal, respectively, but without an examination of their ontogeny and deeper homologies we are likely to be missing important parts of the story that can lead to more nuanced coding schemes.

USING FOSSILS TO RECONSTRUCT PHYLOGENIES

The inclusion of fossil species provided better resolution of phylogenetic relationships in the cassidulids, allowed for the delimitation of supraspecific taxa and detected taxonomic inconsistencies that have not been assessed before. For example, *K. malayana* was classified in the cassidulids (Mooi, 1990b; Suter, 1994b), and many have considered *Rl. pacifica* congeneric with *C. caribaearum* (e.g. Agassiz, 1869; Mortensen, 1948a), but the analyses performed here show that *Rhyncholampas* and *Cassidulus* have been separated for ≥ 60 Myr. Characters responsible for this nesting include: scattered arrangement of phyllopores in posterior phyllodes and convex shape of bourrelet 5, which is shared with *C. mitis* and *C. briareus*, petals with a narrow poriferous zone, a high number of sphaeridia and naked zone with reduced pits, which is shared only with *C. mitis*.

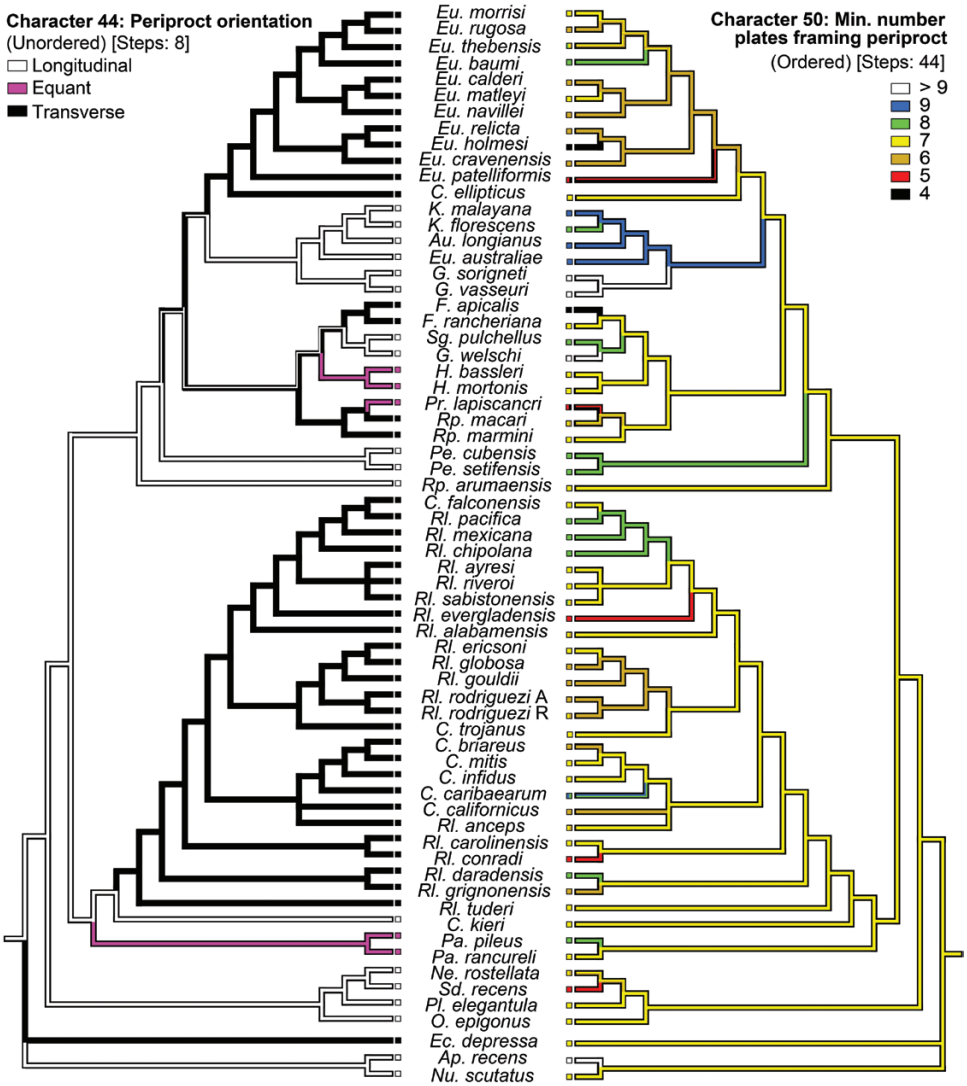

Figure 17. Mirrored trees depicting the maximum parsimony optimization of 'periproct orientation' on the left and 'minimum number of plates framing the periproct' on the right. Branch colour refers to inferred ancestral state.

Smith (2001) and Kroh & Smith (2010) also recovered different results from phylogenies with and without fossils (Fig. 1C, E). As a result of unique combinations of character states that have often been erased in Recent species, fossils generally improve phylogenetic resolution (Huelsenbeck, 1994). However, this improvement will depend on trade-offs between the completeness and temporal position of the fossils. For example, young fossils with low completeness may worsen the phylogenetic resolution (Huelsenbeck, 1991). In the phylogeny reconstructed here, completeness was relatively high (74–100%), but one of the species with lower completeness (*Rl. riveroi*, 75–77% complete) and dating back to the Late Oligocene resulted in a trichotomy, whereas a taxon from the Late Cretaceous with similar completeness (*G. welschi*, 74–75% complete) had a better resolution.

Fossils may not be as important when recovering the relationships of very closely related extant taxa or of taxa whose diversity trajectories are skewed towards the recent. However, because the diversity trajectory of cassiduoids is bottom heavy and its few extant species are relicts, descending from ancient lineages separated by tens of millions of years, adding fossils is necessary to recover the morphological information lost since those lineages split. Phylogenetic studies that include fossil invertebrates are still uncommon for numerous reasons, including the incompleteness and lack of knowledge of the fossil record, the physical separation of biological and palaeontological collections, and

the different research traditions between these two disciplines. Also, although the resolution of the present analysis has not been diminished by the amount of missing data, their negative effect in phylogenetic resolution usually prevents the inclusion of fossil taxa in evolutionary studies (Donoghue *et al.*, 1989). As observed here, the effect of missing data can be reduced if more characters are added (Wiens, 2003; Prevosti & Chemisquy, 2010) even if they are highly homoplastic. Our results strongly recommend the inclusion of fossil taxa whenever possible.

ACKNOWLEDGEMENTS

This work was supported in part by the Philip Sandford Boone Chair in Paleontology. We are thankful to Andreas Kroh and an anonymous reviewer for providing detailed and insightful feedback that greatly improved the quality of the manuscript. Angela Zanata, Cynthia Manso and Kipling Will are thanked for helpful comments on an earlier version of the manuscript, and Roger W. Portell for help with deciphering the age of Cuban outcrops. Ross Pogson and Stephen Keable (AM), Cathy Groves and Gordon Hendler (LACM), Austin Hendy and Kathryn Estes-Smargiassi (LACMIP), Emese Bodor, László Makádi, Palotás Klára and Zoltán Lantos (MBFSZ), Adam J. Baldinger and Gonzalo Giribet (MCZ), Lionel Cavin and Pierre-Alain Proz (MHNG GEPI), Anouchka Sato, Jocelyn Falconnet, Marc P. Eléaume and Sylvain Charbonnier (MNHN), Renato Ventura (MNRJ), Jolanta Jurkowska (MP MNHWU), David Holloway, Frank Holmes, Melanie Mackenzie and Tim O'Hara (MV), Andrew Cabrinovic and Timothy Ewin (NHMUK), Andreas Kroh (NHMW), Walter Etter (NMB), Chad Walter, Jennifer Strotman, Jon Norenburg, Kathy Hollis and Mark Florence (USNM), Sabine Stöhr (SMNH), Gustav Paulay, John D. Slapcinsky, Roger W. Portell (UF), Cynthia Manso (UFISITAB), Joke Bleeker (Naturalis Biodiversity Center), Carsten Lüter (ZMB), Jørgen Olesen and Tom Schiøtte (ZMUC) and Michela Borges (ZUEC) are thanked for granting access to museum collections and/or sending specimens on loan and/or sending images of specimens and/or providing literature. We also thank Dula Parkinson and Harold Barnard (ALS-LBNL) for technical support to generate the SRμCT imagery. This study was funded by the Systematics Research Fund (the Systematics Association and the Linnean Society of London), the Leeper Fund and the Robert and Nancy Beim Endowed Graduate Field Research Fund (Department of Integrative Biology, University of California, Berkeley), the UCMP Annie Alexander Fund and the Palmer Fund (UCMP), the Berkeley Chapter of Sigma Xi, the UF's Emily H. and Harold E. Vokes Grants-in-Aid for collection-based invertebrate palaeontology research and the 2016 NHM IP Collections Study Grant (LACMIP). The research also benefitted from a grant by the French state managed by the Agence Nationale de la Recherche via the programme 'Investissements d'avenir' (ANR-11-INBS-0004-RECOLNAT) and used resources of the Advanced Light Source, which is a DOE Office of Science User Facility under contract number DE-AC02-05CH11231.

REFERENCES

Academia de Ciencias de Cuba. **1988.** *Mapa geológico de Cuba, escala 1:250,000*. Havana: El Instituto.

Adegoke, OS. 1977. Stratigraphy and paleontology of the Ewekoro Formation (Paleocene) of southwestern Nigeria. *Bulletin of American Paleontology* **71:** 5–379.

Afzal J, **Williams M**, **Aldridge RJ. 2009.** Revised stratigraphy of the lower Cenozoic succession of the Greater Indus Basin in Pakistan. *Journal of Micropalaeontology* **28:** 7–23.

Agassiz A. 1863. List of the echinoderms sent to different institutions in exchange for other specimens, with annotations. *Bulletin of the Museum of Comparative Zoology* **1:** 17–28.

Agassiz A. 1869. Preliminary report on the Echini and starfishes dredged in deep water between Cuba and the Florida Reef, by L. F. de Pourtalès, Assist. U.S. Coast Survey. *Bulletin of the Museum of Comparative Zoölogy at Harvard College* **1:** 253–308.

Agassiz A. 1872. Revision of the Echini. *Memoirs of the Museum of Comparative Zoology at Harvard College* **3:** 1–378.

Agassiz A. 1879. Preliminary report on the Echini of the exploring expedition of H.M.S "Challenger". *Proceedings of the American Academy of Arts and Sciences* **6:** 190–212.

Agassiz L. 1839. Description des Échinodermes fossiles de la Suisse. Première partie, Spatangoides et Clypéasteroides. *Mémoires de la Société Helvétique des Sciences Naturelles* **3:** 1–101.

Agassiz L, **Desor E. 1847.** Catalogue raisonné des espéces, des genres et des familles d'échinides. *Annales des Sciences Naturelles, Zoologie, série 3* **7:** 129–168.

d'Archiac E, **Haime J. 1853.** *Description des animaux fossiles du groupe nummulitique de l'Inde*. Paris: Gide et Baudry.

Arnold BW, **Clark HL. 1927.** Jamaican fossil Echini; with descriptions of new species of Cenozoic Echinoidea by H. L. Hawkins. *Memoirs of the Museum of Comparative Zoology* **50:** 1–84.

Baker AN. 1983. A new apatopygid echinoid genus from New Zealand (Echinodermata: Cassiduloida). *National Museum of New Zealand Records* **2:** 163–173.

Barras CG. 2008. Morphological innovation associated with the expansion of atelostomate irregular echinoids into fine-grained sediments during the Jurassic. *Palaeogeography, Palaeoclimatology, Palaeoecology* **263:** 44–57.

Bell MA, **Lloyd GT. 2015.** strap: an R package for plotting phylogenies against stratigraphy and assessing their stratigraphic congruence. *Palaeontology* **58:** 379–389.

Benton MJ, **Storrs GW. 1994.** Testing the quality of the fossil record: paleontological knowledge is improving. *Geology* **22:** 111–114.

Besaire H, **Lambert J. 1930.** Notes sur quelques Échinides de Madagascar et du Zululand. *Bulletin de la Société Géologique de France, série 4* **30:** 107–117.

Bittner A. 1892. Über Echiniden des Tertiärs von Australien. *Sitzungsberichte der Kaiserliche Akademie der Wissenschaften, mathematisch-naturwissenschaftliche Classe, Band Abtheilung I* **101:** 331–371.

Bodenbender BE, **Fisher EC. 2001.** Stratocladistic analysis of blastoid phylogeny. *Journal of Paleontology* **75:** 351–369.

Boivin S, **Saucède T**, **Laffont R**, **Steimetz E**, **Neige P. 2018.** Diversification rates indicate an early role of adaptive radiations at the origin of modern echinoid fauna. *PLoS ONE* **13:** e0194575.

Carrasco JF. 2016. *Rhyncholampas grignonensis* (Defrance, 1825) (Echinoidea, Eoceno) in Spain. Review of synonymy. *Batalleria* **23:** 35–41.

Carter BD, **Beisel TH. 1987.** "*Cassidulus trojanus*" belongs in the genus *Eurhodia* (Echinoidea) based upon new criteria. *Journal of Palaeontology* **61:** 1080–1083.

Coates AG. 1999. Lithostratigraphy of the Neogene strata of the Caribbean coast from Limon, Costa Rica, to Colon, Panamá. In: Collins LS, Coates AG, eds. *A paleobiotic survey of Caribbean faunas from the Neogene of the Isthmus of Panama*. Ithaca: Paleontological Research Institution, 17–38.

Cohen KM, **Finney SC**, **Gibbard PL**, **Fan J-X. 2013.** The ICS International Chronostratigraphic Chart. V2017/02 (updated). *Episodes* **36:** 199–204.

Cooke CW. 1942. Cenozoic irregular echinoids of eastern United States. *Journal of Paleontology* **16:** 1–62.

Cooke CW. 1953. American upper Cretaceous Echinoidea. *Geological Survey Professional Paper* **254–A:** 1–44.

Cooke CW. 1955. Some Cretaceous echinoids from the Americas. *Geological Survey Professional Paper* **264–E:** 1–112.

Cooke CW. 1959. Cenozoic echinoids of eastern United States. *Geological Survey Professional Paper* **321:** 1–106.

Cooke CW. 1961. Cenozoic and Cretaceous echinoids from Trinidad and Venezuela. *Smithsonian Miscellaneous Collections* **142:** 1–35.

Cotteau G. 1866. Échinides nouveaux ou peu connus. *Revue et Magasin de Zoologie Pure et Appliquée, série 2* **18:** 262–268.

Cotteau G. 1883. Échinides nouveaux ou peu connus, part II. *Bulletin de la Société Zoologique de France* **8:** 450–464.

Cotteau G. 1885–1889. *Paléontologie française. Terrain Tertiaire. Échinides Eocènes, Vol.* **1**. Paris: G. Masson.

Day MO, **Rubidge BS**, **Abdala F. 2016.** A new mid-Permian burnetiamorph therapsid from the Main Karoo Basin of South Africa and a phylogenetic review of Burnetiamorpha. *Acta Palaeontologica Polonica* **61:** 701–719.

Döderlein L. 1906. Die Echinoiden der Deutschen Tiefsee-Expedition. In: Chun C, ed. *Wissenschaftliche Ergebnisse der Deutschen Tiefsee-Expedition auf dem Dampfer "Valdivia" 1898–1899*. Jena: Gustav Fischer, 61–290.

Donoghue MJ, **Doyle JA**, **Gauthier J**, **Kluge AG**, **Rowe T. 1989.** The importance of fossils in phylogeny reconstruction. *Annual Review of Ecology and Systematics* **20:** 431–460.

Donovan SK. 2004. Echinoderms of the mid-Cainozoic White Limestone group of Jamaica. *Cainozoic Research* **3:** 143–156.

Duncan PM. 1877. On the Echinodermata of the Australian Cenozoic (Tertiary) deposits. *Quarterly Journal of the Geological Society of London* **33:** 43–73.

Duncan PM, **Sladen WP. 1882.** Fossil Echinoidea of western Sind and the coast of Bilúchístán and of the Persian Gulf, from the Tertiary Formations. Fasc. II. Echinoidea from the Ranikot series of western Sind. *Palaeontologica Indica, série 14* **1:** 21–100.

Felsenstein J. 1985. Confidence limits on phylogenies: an approach using the bootstrap. *Evolution* **39:** 783–791.

Fischer AG. 1951. The echinoid fauna of the Inglis member, Moodys Branch formation. *Florida Geological Survey B* **34:** 49–101.

Fisher DC. 2008. Stratocladistics: integrating temporal data and character data in phylogenetic inference. *Annual Review of Ecology, Evolution, and Systematics* **39:** 365–85.

Fourtau R. 1899. Révision des échinides fossiles de l'Egypt. *Mémoires de l'Institut Egyptien (Le Caire)* **3:** 605–740.

Fourtau R. 1913. *Catalogue des invertébrés fossiles de l'Egypte représentés dans les collections du Géological Museum au Caire. Terrains Tertiaires, Ière partie. Échinides Eocènes.* Cairo: Gouvernement Égyptien, Administration des Arpentages.

Fox DL, **Fisher DC**, **Leighton LR. 1999.** Reconstructing phylogeny with and without temporal data. *Science* **284:** 1816–1819.

Gauthier J, **Kluge AG**, **Rowe T. 1988.** Amniote phylogeny and the importance of fossils. *Cladistics* **4:** 105–209.

Goubert ME. 1859. Quelques mots sur l'étage Eocène Moyen dans le bassin de Paris. *Bulletin de la Société Géologique de France, série 2* **17:** 137–148.

Gregory JW. 1892. Further additions to Australian fossil Echinoidea. *Geological Magazine* **9:** 433–438.

Holmes FC. 2004. A new Late Eocene cassiduloid (Echinoidea) from Yorke Pensilvania, South Australia. *Memoirs of Museum Victoria* **61:** 209–216.

Huelsenbeck JP. 1991. When fossils are better than extant taxa in phylogenetic analysis. *Systematic Zoology* **40:** 458–469.

Huelsenbeck JP. 1994. Comparing the stratigraphic record to estimates of phylogeny. *Paleobiology* **20:** 470–483.

Jeannet A. 1928. Contribution á l'étude des échinides tertiaires de la Trinité et du Venezuela. *Mémories de la Société Paléontologique Suisse* **48:** 1–49.

Kellum LB. 1926. Paleontology and stratigraphy of the Castle Hayne and Trent Marls in North Carolina. *United States Geological Survey* **143:** 1–41.

Kew WSW. 1920. Cretaceous and Cenozoic Echinoidea of the Pacific Coast of North America. *University of California Publications in Geological Sciences* **12:** 22–236.

Kier PM. 1962. Revision of the cassiduloid echinoids. *Smithsonian Miscellaneous Collections* **144:** 1–262.

Kier PM. 1963. Tertiary echinoids from the Caloosahatchee and Tamiami Formations of Florida. *Smithsonian Miscellaneous Collections* **145:** 1–63.

Kier PM. 1972. Tertiary and Mesozoic echinoids of Saudi Arabia. *Smithsonian Contributions to Paleobiology* **10:** 1–242.

Kier PM. 1974. Evolutionary trends and their functional significance in the post-Paleozoic echinoids. *Memoir (The Paleontological Society)* **5:** 1–95.

Kier PM. 1980. The echinoids of the middle Eocene Warley Hill formation, Santee Limestone and Castle Hayne Limestone of North and South Carolina. *Smithsonian Contributions to Paleobiology* **39:** 1–102.

Kier PM, **Lawson MH. 1978.** Index of living and fossil echinoids 1924–1970. *Smithsonian Contributions to Paleobiology* **34:** 1–182.

Krau L. 1954. Nova espécie de ouriço do mar: *Cassidulus mitis*, Ordem Cassiduloida, Echinoidea, capturado na Baía de Sepetiba. *Memórias do Instituto Oswaldo Cruz* **52:** 455–475.

Kroh A, **Mooi R. 2018.** *Neognathostomata*. Available at: http://www.marinespecies.org/aphia.php?p=taxdetails&id=510501

Kroh A, **Smith AB. 2010.** The phylogeny and classification of post-Palaeozoic echinoids. *Journal of Systematic Palaeontology* **8:** 147–212.

Lambert J. 1905. Notes sur quelques Échinides éocéniques de l'Aude et de l'Hérault. In: Doncieux L, ed. Catalogue descriptif des fossiles nummulitiques de l'Aude et de l'Hérault. *Annales de l'Université de Lyon, Nouvelle série, I. Sciences, Médecine* **17:** 129–164.

Lambert J. 1931. Étude sur les échinides fossiles du Nord de l'Afrique. *Memoires de la Societe Geologique de France, Nouvelle serie (Mémoire No. 16)* **7:** 5–108.

Lambert J. 1933. Échinides de Madagascar communiques par M. H. Besairie. *Annales Geologiques du Service des Mines* **3:** 1–49.

Lambert J. 1937. Échinides fossiles du Maroc. *Notes et Memoires du Service des Mines et de la Carte Geologique du Maroc* **39:** 39–109.

Lodeiros C, **Martín A**, **Francisco V**, **Noriega N**, **Díaz Y**, **Reyes J**, **Aguilera O**, **Alió J. 2013.** Echinoderms from Venezuela: scientific recount, diversity and distribution. In: Alvarado JJ, Solís-Marín FA, eds. *Echinoderm research and diversity in Latin America*. Heidelberg: Springer, 235–276.

de Loriol P. 1880. Monographie des échinides contenus dans les Couches Nummultiques de l'Egypte. *Memoires de la Societe Physique d'Histoire Naturelle, Geneve* **27:** 59–148.

Lovén S. 1874. Études sur les échinoidées. *Kongelige Svenska Vetenskaps-Akademiens Handlingar* **11:** 1–91.

Maddison WP, **Maddison DR. 2018.** *Mesquite: a modular system for evolutionary analysis. Version 3.51.* Available at: http://www.mesquiteproject.org

Mansfield WC. 1932. Pliocene fossils from limestone in Southern Florida. *Geological Survey Professional Paper* **170D:** 43–56.

McCrady J. 1859. Remarks on the Eocene Formation in the neighborhood of Alligator, Florida. *Proceedings of the Elliott Society of Natural History (Charleston, South Carolina)* **1:** 282–283.

McKinney ML, **Oyen CW. 1989.** Causation and nonrandomness in biological and geological time series: temperature as a proximal control of extinction and diversity. *Palaios* **4:** 3–15.

Meunier S. 1906. Observation sur la géologie du Sénégal. *Le Naturaliste* **471:** 233–235.

Mihaljević M, **Klug C**, **Aguilera O**, **Lüthi T**, **Sánchez-Villagra MR. 2010.** Paleodiversity of Caribbean echinoids including new material from the Venezuelan Neogene. *Palaeontologia Electronica* **13:** 13.3.20A.

Mooi R. 1990a. A new "living fossil" echinoid (Echinodermata) and the ecology and paleobiology of Caribbean cassiduloids. *Bulletin of Marine Science* **46:** 688–700.

Mooi R. 1990b. Living cassiduloids (Echinodermata: Echinoidea): a key and annotated list. *Proceedings of the Biological Society of Washington* **103:** 63–85.

Mortensen T. 1948a. *A monograph of the Echinoidea. IV. 1. Holectypoida, Cassiduloida*. Copenhagen: C. A. Reitzel.

Mortensen T. 1948b. New Echinoida (Cassiduloida; Clypeasteroida). *Videnskabelige Meddelelser Dansk Naturhistorisk Forening* **111:** 67–72.

Néraudeau D, **Mazet M**, **Roman J. 1997.** La faune d'échinides du Lutétien de Cahaignes (Eure, France). *Cossmanniana* **4:** 29–38.

O'Leary MA, **Kaufman SG. 2012.** *MorphoBank 3.0: Web application for morphological phylogenetics and taxonomy*. Available at: http://www.morphobank.org

d'Orbigny A. 1853–1860. *Paléontologie française. Description des animaux invertébrés. Terrains Crétacés. Échinoïdes irréguliers*, *Vol.* **6**. Paris: G. Masson.

Osborn AS, **Ciampaglio CN. 2014.** *Rhyncholampas alabamensis* (Twitchell) (Echinoidea, Cassidulidae) from the Late Oligocene (Chattian) Chickasawhay Limestone of Mississippi and Alabama. *Southeastern Geology* **50:** 135–143.

Osborn AS, **Mooi R**, **Ciampaglio CN. 2016.** Additions to the Eocene echinoid fauna of the southeastern United States, including a new genus and species of prenasterid heart urchin. *Southeastern Geology* **52:** 33–59.

Oyen CW, **Portell RW. 1996.** A new species of *Rhyncholampas* (Echinoidea: Cassidulidae) from the Chipola Formation: the first confirmed member of the genus from the Miocene of the southeastern USA and the Caribbean. *Tulane Studies in Geology and Paleontology* **29:** 59–66.

Oyen CW, **Portell RW. 2002.** Oligocene and Miocene echinoids. *Florida Fossil Invertebrates* **2:** 1–22.

Philip GM. 1963. Two Australian Tertiary neolampadids, and the classification of the cassiduloid echinoids. *Palaeontology* **6:** 106–107.

Pol D, **Norell MA. 2001.** Comments on the Manhattan stratigraphic measure. *Cladistics* **17:** 285–289.

Prevosti FJ, **Chemisquy MA. 2010.** The impact of missing data on real morphological phylogenies: influence of the number and distribution of missing entries. *Cladistics* **26:** 326–339.

Ravenel E. 1848. *Echinidae recent and fossil, of South-Carolina*. Charleston: Burges & James.

Roman J, **Gorodiski A. 1959.** Échinides Éocènes du Sénégal. *Notes du Service de Géologie et de Prospection Minière* **3:** 1–91.

Roman J, **Strougo A. 1994.** Echinoides du Libyen (Eocene Inférieur) d'Egypte. *Revue de Paleobiologie* **13:** 29–57.

Rowe T. 1988. Definition, diagnosis and origin of Mammalia. *Journal of Vertebrate Paleontology* **8:** 241–264.

Sánchez Roig M. 1926. Contribucion a la Paleontologia Cubana: los equinodermos fosiles de Cuba. *Boletin de Minas* **10:** 1–179.

Sánchez Roig M. 1949. Los equinodermos fosiles de Cuba. *Paleontologia Cubana* **1:** 1–330.

Sánchez Roig M. 1952. Nuevos generos y especies de equinodermos fosiles cubanos. *Memorias de la Sociedad Cubana de Historia Natural "Felipe Poey"* **21:** 1–61.

Saucède T, **Mooi R**, **David B. 2003.** Combining embryology and paleontology: origins of the anterior-posterior axis in echinoids. *Comptes Rendus Palevol* **2:** 399–412.

Saucède T, **Néraudeau D. 2006.** An "Elvis" echinoid, *Nucleopygus* (*Jolyclypus*) *jolyi*, from the Cenomanian of France: phylogenetic analysis, sexual dimorphism and neotype designation. *Cretaceous Research* **27:** 542–554.

Siddall ME. 1998. Stratigraphic fit to phylogenies: a proposed solution. *Cladistics* **14:** 201–208.

Smiser JS. 1935. A monograph of the Belgian Cretaceous Echinoids. *Mémoires du Musée Royal d'Histoire Naturelle de Belgique* **68:** 1–98.

Smith AB. 1994. *Systematics and the fossil record*. London: Blackwell Scientific.

Smith AB. 2000. Stratigraphy in phylogeny reconstruction. *Journal of Paleontology* **74:** 763–766.

Smith AB. 2001. Probing the cassiduloid origins of clypeasteroid echinoids using stratigraphically restricted parsimony analysis. *Paleobiology* **27:** 392–404.

Smith AB, **Jeffery CH. 1998.** Selectivity of extinction among sea urchins at the end of the Cretaceous period. *Nature* **392:** 69–71.

Smith AB, **Jeffery CH. 2000.** Maastrichtian and Paleocene echinoids: a key to world faunas. *Special Papers in Palaeontology* **63:** 1–406.

Smith AB, **Wright CW. 2000.** British Cretaceous echinoids. Part 6, Neognathostomata (Cassiduloids). *Monographs of the Palaeontographical Society* **154:** 391–429.

Souto C, **Manso CLC**, **Martins L. 2011.** Rediscovery and redescription of *Cassidulus infidus* (Echinoidea: Cassidulidae) from northeastern Brazil. *Zootaxa* **3095:** 39–48.

Souto C, **Martins L. 2018.** Synchrotron micro-CT scanning leads to the discovery of a new genus of morphologically conserved echinoid (Echinodermata: Cassiduloida). *Zootaxa* **4457:** 70–92.

Squires RL, **Demetrion RA. 1995.** A new genus of cassiduloid echinoid from the Lower Eocene of the Pacific Coast of western North America and a new report of *Cassidulus ellipticus* Kew, 1920, from the Lower Eocene of Baja California Sur, Mexico. *Journal of Paleontology* **69:** 509–515.

Srivastava DK, **Singh AP**, **Tiwari RP**, **Jauhri AK. 2008.** Cassiduloids (Echinoidea) from the Siju Formation (Late Lutetian–Early Bartonian) of the south Garo Hills, Meghalaya, India. *Revue de Paléobiologie, Genève* **27:** 511–523.

Sumrall CD, **Brochu CA. 2003.** Resolution, sampling, higher taxa and assumptions in stratocladistic analysis. *Journal of Paleontology* **77:** 189–194.

Suter SJ. 1988. The decline of the cassiduloids: merely bad luck? In: Burke RD, Mladenov PV, Lambert P, Parsley RL, eds. *Echinoderm biology*. Rotterdam: Balkema, 91–95.

Suter SJ. 1994a. Cladistic analysis of cassiduloid echinoids: trying to see the phylogeny for the trees. *Biological Journal of the Linnean Society* **52:** 31–72.

Suter SJ. 1994b. Cladistic analysis of the living cassiduloids (Echinoidea), and the effects of character ordering and successive approximations weighting. *Zoological Journal of the Linnean Society* **112:** 363–387.

Swofford DL. 2003. *PAUP*. Phylogenetic analysis using parsimony (*and other methods). Version 4.0a163*. Sunderland: Sinauer Associates.

Tawadros EE. 2012. *Geology of North Africa*. Leiden: CRC Press, Balkema.

Tessier F, **Roman J. 1973.** Études paléontologiques et géologiques sur les Falaises de Fresco (Côte d'Ivorie). 6, Échinides. *Annales de la Faculté des Sciences, Dakar* **26:** 139–172.

Vermeij GJ. 1977. The Mesozoic marine revolution: evidence from snails, predators and grazers. *Paleobiology* **3:** 245–258.

Wagner PJ. 2000. Exhaustion of morphologic character states among fossil taxa. *Evolution* **54:** 365–386.

Weisbord NE. 1934. Some Cretaceous and Tertiary echinoids from Cuba. *Bulletins of American Paleontology* **20:** 1–84.

Wiens JJ. 2003. Missing data, incomplete taxa, and phylogenetic accuracy. *Systematic Biology* **52:** 528–538.

Wilkinson M, **Suter SJ**, **Shires VL. 1996.** The reduced cladistic consensus method and cassiduloid echinoid phylogeny. *Historical Biology* **12:** 63–73.

Wills MA. 1999. Congruence between stratigraphy and phylogeny: randomization tests and the gap excess ratio. *Systematic Biology* **48:** 559–580.

Wills MA, **Barrett PM**, **Heathcote JF. 2008.** The modified gap excess ratio (GER*) and the stratigraphic congruence of dinosaur phylogenies. *Systematic Biology* **57:** 891–904.

SUPPORTING INFORMATION

Additional Supporting Information may be found in the online version of this article at the publisher's web-site:

Appendix S1. Data matrix of 66 taxa and 98 characters. Partial uncertainty is coded within curly brackets and polymorphism within brackets. Missing data are indicated by '?' and inapplicability by '–'. Species nomenclature follows works before this analysis. Numbers in bold on the top of the column indicate the character in each block. NEXUS format [available in MorphoBank (O'Leary & Kaufman, 2012), project P3287].
Appendix S2. Commands for phylogenetic analyses and estimation of stratigraphic congruence metrics [available in MorphoBank (O'Leary & Kaufman, 2012), project P3287]. Modifications among PAUP analyses are in square brackets; file names (in red) were also modified according to the analysis performed.
Appendix S3. Strict consensus and 50% majority-rule consensus of 900 MPTs recovered by analysis 1 (including all taxa, all characters and partial uncertainty) with unordered characters (724 steps, CI 0.246, RI 0.610). Extant taxa are in bold. Commands for phylogenetic analysis are after cladograms.
Appendix S4. Single MPT recovered by analysis 1 (including all taxa, all characters and partial uncertainty) with reweighted characters (reweighting based on rescaled consistency index; CI 0.357, RI 0.736). Extant taxa are in bold. Character weight, stratigraphic fit metrics and PAUP commands for phylogenetic analysis follow the cladogram.
Appendix S5. Stratigraphic fit for each MPT estimated by the following metrics: the gap excess ratio (GER; Wills, 1999; Wills *et al.*, 2008), the modified Manhattan stratigraphic measure (MSM*; Siddall, 1998; Pol & Norell, 2001), the relative consistency index (RCI; Benton & Storrs, 1994) and the stratigraphic consistency index (SCI; Huelsenbeck, 1994). Estimated P-values for each metric (est.p.) are also included. Best-fitting values for each metric are in bold.
Appendix S6. Character attributes: character number (Ch.), number of character states (#states), percentage of missing data (MD; lower values, when present, consider partial uncertainty as missing data), number of steps (#steps) and consistency index (CI). Characters shaded in grey have a high percentage of missing data and were removed from analysis 2.